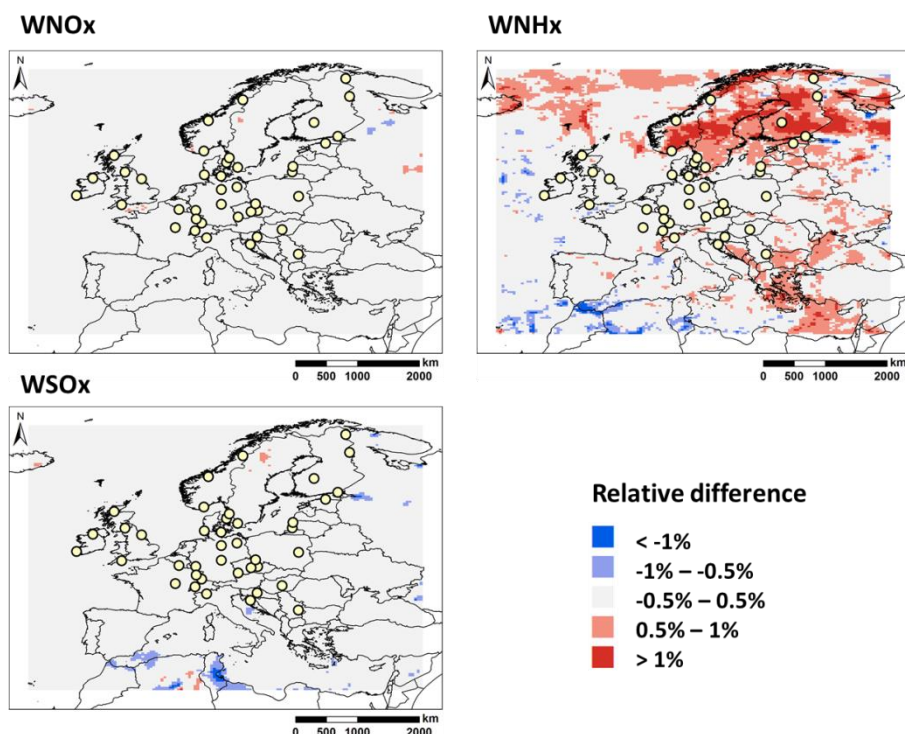


## S1 Analysis of the errors in wet deposition due to errors in the primary particulate matter emissions

Errors were found in the emissions of primary particulate matter for Russia and North African countries and shipping for the period 1991-1999. Unfortunately it was not possible to re-run the simulations since these errors were not detected until late in the data analysis. In order to estimate the impact on the wet deposition estimates, the CHIMERE model was used to simulate wet deposition using the incorrect and corrected emissions for 1998, the year for which the emission error is the largest. Figure S1 shows the relative errors in the model estimates of WNOx, WNHx and WSOx as a result of the errors in emissions. Errors in WNOx and WSOx were less than 0.5% in most of the domain with maximum errors of 0.95% and 1.5%, respectively. Errors in WNHx were also mostly below 0.5% but larger errors were estimated for about a quarter of the domain (mostly in the northeast), with a maximum error of 2.4%. These errors are small compared with the overall uncertainty of the model estimates and the uncertainty of the observations. Errors in the trends calculated from the simulations with erroneous emissions are expected to be smaller than the errors in annual deposition rates. From this analysis we conclude that the error in emissions is unlikely to affect the results and conclusions of the study significantly.



**Figure S1: Maps of relative difference between the model estimates of WNOx, WNHx and WSOx for the simulations using the original (incorrect) emissions and those using the corrected emissions of primary PM in Russia, North Africa and maritime areas for 1998. Circles show the locations of the sites used to evaluate modelled deposition. Note: Positive values indicate that the emission error resulted in larger values of wet deposition and vice versa.**

**S2 Table and Figures cited in the article**

**Table S1: Main features of the chemistry-transport models involved in the EURODELTA-Trends deposition modelling exercise**  
 (Adapted from Colette et al., 2017a).

| Model   | CHIMERE (CHIM)               | CMAQ                                | EMEP MSC-W (EMEP)                     | LOTOS-EUROS (LOTO)                       | MATCH   | MINNI                               |
|---|------------------------------|-------------------------------------|---------------------------------------|--|---|-------------------------------------|
| <b>Version / Date</b>                                   | Modified CHIMERE2013         | V5.0.2                              | rv4.7 spring 2015                     | v1.10.005                                | VSOA April 2016                                     | V4.7                                |
| <b>Operator</b>   | INERIS                       | BSC                                 | MET Norway                            | TNO                                      | SMHI  | ENEA/Arianet S.r.l.                 |
| <b>Name and resolution of the meteorological driver</b> | WRF (common driver)<br>0.44° | WRF<br>25 km                        | WRF (common driver)<br>0.44°          | RACMO2<br>0.22°                          | HIRLAM EURO4M reanalysis<br>Approx. 22 km           | WRF (common driver)<br>0.44°        |
| <b>Vertical layers</b>                                  | 9 sigma                      | 15 sigma                            | 20 sigma                              | 5 (4 dynamic layers and a surface layer) | 39 hybrid levels of the meteorological model layers | 16 fixed terrain-following layers   |
| <b>Vertical extent</b>                                  | 500 hPa                      | 50 hPa                              | 100 hPa                               | 5000 m                                   | ca. 5000 m (4700–6000 m)                            | 10 000m                             |
| <b>Surface concentration</b>                            | First model level            | First model level                   | Downscaled to 3 m                     | Downscaled to 3 m                        | Downscaled to 3 m                                   | First model level                   |
| <b>Land-use database</b>                                | GLOBCOVER (24 classes)       | Corine Land Cover 2006 (44 classes) | CCE/SEI for Europe, elsewhere GLC2000 | Corine Land Cover 2000 (13 classes)      | CCE/SEI for Europe                                  | Corine Land Cover 2006 (22 classes) |

| Model                              | CHIMERE (CHIM)                                 | CMAQ  | EMEP MSC-W (EMEP)  | LOTOS-EUROS<br>(LOTO)  | MATCH  | MINNI   |
|------------------------------------|--|---|--|--|--|---|
| <b>Dry deposition</b>              | Resistance model (Emberson et al., 2000a, b)   | Resistance model (Venkatram and Pleim, 1999)    | Resistance model for gases (Venkatram and Pleim, 1999); for aerosols: Simpson et al. (2012)          | Resistance model, DEPAC3.11 for gases, Van Zanten et al. (2010) and Zhang et al. (2001) for aerosols | Resistance model depending on aerodynamic resistance and land use (vegetation). Similar to Andersson et al. (2007)                         | Resistance model based on Wesely (1989)                               |
| <b>Ammonia compensation points</b> | None   | None  | None, but zero NH <sub>3</sub> deposition over growing crops   | Only for stomatal, external leaf surface and soil (=0))  | None   | None  |
| <b>Stomatal resistance</b>         | Emberson et al. (2000a, b)                     | Wesely (1989)                                   | DO3SEEMEP: Emberson et al. (2000a, b), Tuovinen et al. (2004), Simpson et al. (2012)                 | Emberson et al. (2000a, b)   | Simple, seasonally varying, diurnal variation of surface resistance for gases with stomatal resistance (similar to Andersson et al., 2007) | Wesely (1989)   |
| <b>Wet deposition - gases</b>      | In-cloud and sub-cloud scavenging coefficients | Simple first-order process (Chang et al., 1987) | In-cloud and sub-cloud scavenging coefficients (implicit dependence on solubility and particle size) | Sub-cloud scavenging coefficient (no in-cloud scavenging)  | In-cloud scavenging of some species based on Henry's law constants. Simple in-cloud and sub-cloud scavenging coefficients for other gases. | In-cloud and sub-cloud scavenging coefficients (Simpson et al., 2003) |

| Model                                       | CHIMERE (CHIM)   | CMAQ   | EMEP MSC-W (EMEP)  | LOTOS-EUROS<br>(LOTO)   | MATCH   | MINNI   |
|---|--|--|--|---|---|---|
| <b>Wet deposition – scavenging of gases</b> | <p>In-cloud: Scavenging for O<sub>3</sub>, NO, NO<sub>2</sub>, NO<sub>3</sub>, HNO<sub>3</sub>, HCl, NH<sub>3</sub>, SO<sub>2</sub>, H<sub>2</sub>O<sub>2</sub> and several VOCs (according to their Henry's law constant)</p> <p>Sub-cloud: Scavenging of NH<sub>3</sub>, HNO<sub>3</sub> and HCl by falling drops</p> <p>Menut et al. (2013); Couvidat et al. (2018)</p> | <p>If the gas participates in cloud chemistry:</p> <p>Scavenging depends on Henry's law constants, dissociation constants, and cloud water pH. If not, the model uses the effective Henry's law equilibrium equation to calculate ending concentrations and deposition amounts</p> <p>Byun and Schere (2006)</p> | <p>Scavenging calculated from the gas mixing ratio, precipitation rate and species-specific scavenging ratios.</p> <p>Different scavenging ratios are used for in-cloud and sub-cloud processes</p> <p>Simpson et al. (2012)</p> | <p>Sub-cloud: Scavenging calculated from the gas mixing ratio, precipitation rate and species-specific scavenging ratios.</p> <p>Simpson et al. (2003) and Scott (1978)</p> | <p>Wet scavenging is assumed to be proportional to the precipitation intensity for most gaseous components. For O<sub>3</sub>, hydrogen peroxide (H<sub>2</sub>O<sub>2</sub>) and SO<sub>2</sub>, in-cloud scavenging is calculated by assuming Henry's law equilibrium. Sub-cloud scavenging is neglected for these species. The wet scavenging coefficients for SO<sub>2</sub>, O<sub>3</sub> and H<sub>2</sub>O<sub>2</sub> depend on meteorology. For other species, fixed species-specific coefficients are used.</p> <p>Andersson et al. (2007)</p> | <p>Scavenging calculated from the gas mixing ratio, precipitation rate and species-specific scavenging ratios.</p> <p>Different scavenging ratios are used for in-cloud and sub-cloud processes.</p> <p>Simpson et al. (2003)</p> |
| <b>Wet deposition - particles</b>           | In-cloud and sub-cloud scavenging coefficients   | Simple first-order process (Chang et al., 1987)  | In-cloud and sub-cloud scavenging coefficients (implicit dependence on solubility and particle size)   | Sub-cloud scavenging coefficient (no in-cloud scavenging)   | In-cloud and sub-cloud scavenging. Similar to Simpson et al. (2012)   | In-cloud and sub-cloud scavenging coefficients (Simpson et al., 2003)   |

| Model   | CHIMERE (CHIM)   | CMAQ   | EMEP MSC-W (EMEP)  | LOTOS-EUROS<br>(LOTO)   | MATCH  | MINNI   |
|---|--|--|--|---|--|---|
| <b>Wet deposition – scavenging of particles</b> | <p>In-cloud: particles can be scavenged either by coagulation with cloud droplets or by precipitating drops. Particles also act as cloud condensation nuclei to form new droplets. This latter process of nucleation is the most efficient one in clouds.</p> <p>Sub-cloud: particles are scavenged by raining drops with the deposition flux depending on empirical scavenging coefficients</p> | <p>The accumulation mode and coarse mode aerosols are assumed to be completely absorbed by the cloud and rain water.</p> <p>The Aitken mode aerosols are treated as interstitial aerosol and are slowly absorbed into the cloud/rain water. Only the equilibrium of the sulphate, nitrate, ammonium, and water system is considered.</p> | <p>In-cloud: As gas scavenging above</p> <p>Sub-cloud: Scavenging calculated from the particle mixing ratio, precipitation rate, raindrop fall speed and a size-dependent collection efficiency.</p> | <p>Sub-cloud: Scavenging calculated from the particle mixing ratio, precipitation rate, raindrop fall speed and a size-dependent collection efficiency.</p> <p>Simpson et al. (2003) and Scott (1978)</p> | <p>In-cloud scavenging is proportional to the fraction of the cloud water that hits the ground as precipitation. All particulate sulphate inside clouds is assumed to be dissolved to cloud droplets. The wet scavenging coefficients for ammonium sulphate and <math>\text{SO}_4^{2-}</math> depend on meteorology. Sub-cloud scavenging for sulphate is calculated as in Berge (1993).</p> | <p>In-cloud: As gas scavenging above</p> <p>Sub-cloud: Scavenging calculated from the particle mixing ratio, precipitation rate, raindrop fall speed and a size-dependent collection efficiency.</p> <p>Simpson et al. (2003)</p> |
| <b>Gas-phase chemistry</b>                      | MELCHIOR2  | CB-05 with chlorine chemistry extensions (Yarwood et al., 2005)  | EmChem09 (Simpson et al., 2012)  | TNO-CBM-IV  | Based on EMEP (Simpson et al., 2012), with modified isoprene chemistry (Carter, 1996; Langner et al., 1998)  | SAPRC99 (Carter, 2000)  |

| Model                               | CHIMERE (CHIM)  | CMAQ  | EMEP MSC-W (EMEP)   | LOTOS-EUROS<br>(LOTO)  | MATCH  | MINNI   |
|-------------------------------------|---|---|---|--|--|---|
| <b>Cloud chemistry</b>              | Aqueous SO <sub>2</sub> chemistry and pH-dependent SO <sub>2</sub> chemistry  | Aqueous SO <sub>2</sub> chemistry (Walcek and Taylor, 1986) | Aqueous SO <sub>2</sub> chemistry, pH-dependent   | Aqueous SO <sub>2</sub> chemistry, pH-dependent (Banzhaf et al., 2012)                               | Aqueous SO <sub>2</sub> chemistry  | Aqueous SO <sub>2</sub> chemistry (Seinfeld and Pandis, 1998) |
| <b>Coarse nitrate</b>               | No reaction with Ca even if reaction with Na is taken into account. Coarse nitrate might exist with transfer from smaller particles                                   | None  | Two formation rates of coarse NO <sub>3</sub> from HNO <sub>3</sub> for relative humidity below/above 90% | Heterogeneous reaction of HNO <sub>3</sub> with coarse sea salt aerosols to obtain NaNO <sub>3</sub> | Transfer of HNO <sub>3</sub> (g) to aerosol nitrate using rate from Strand and Hov (1994)<br><br>Wichink Kruit et al. (2012) | None  |
| <b>Ammonium nitrate equilibrium</b> | ISORROPIA v2.1 (Nenes et al., 1999)   | ISORROPIA v2.1 (Nenes et al., 1999)                         | MARS (Binkowski and Shankar, 1995)  | ISORROPIA v2 (Nenes et al., 1999)  | RH- & T-dependent equilibrium constant (Mozurkewich, 1993)   | ISORROPIA v1.7 (Nenes et al., 1999)                           |
| <b>Aerosol physics</b>              | Coagulation/ condensation/ nucleation<br>Computation of the wet diameter for each size bin as a function of humidity (used for coagulation, condensation, deposition) | Coagulation/ condensation/ nucleation                       | Not used here   | Not used here  | Not used here  | Coagulation/ condensation/ nucleation                         |

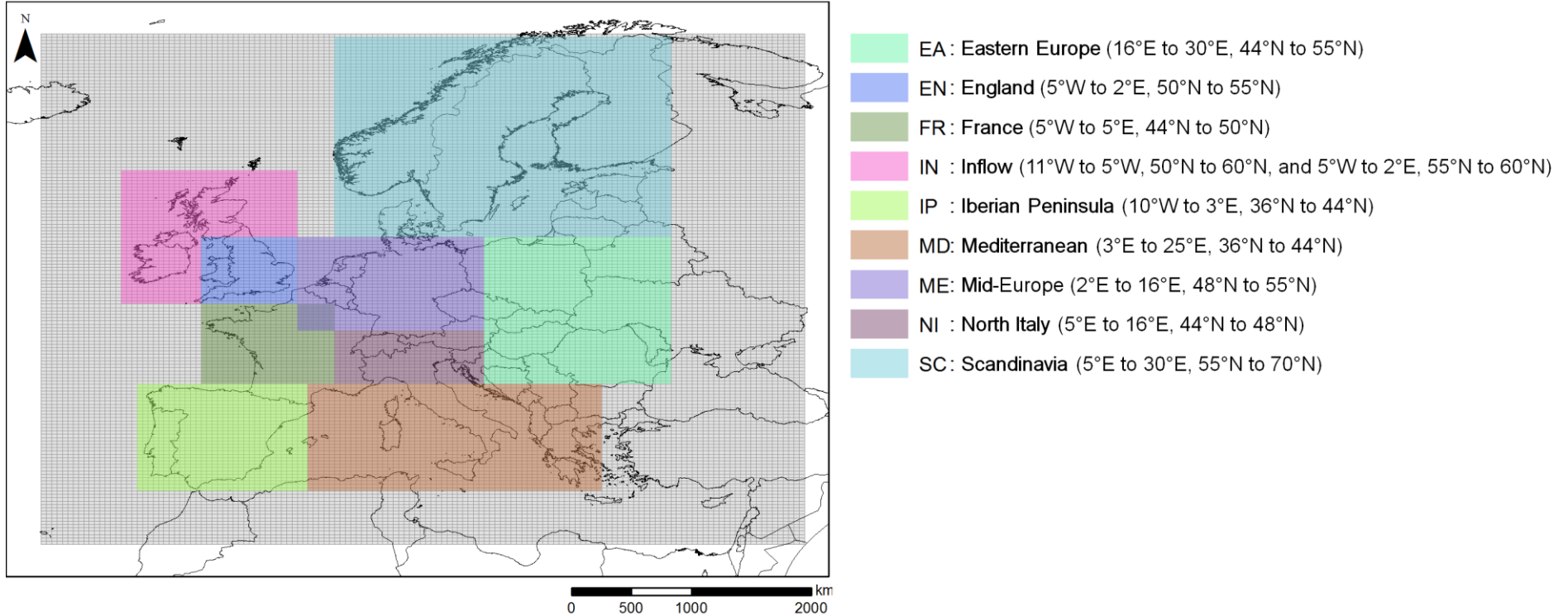


**Figure S2: Map showing the grid cells of the modelling domain and the nine sub-regions used in the trend attribution analyses.**

**Table S2: EMEP stations used for the observations of the various wet deposition and concentration components**

| Station | Latitude | Longitude | WNOx | WNHx | WSOx | TNO3 | TNH4 | TSO4 | Extra site (2000-2010) |
|---------|----------|-----------|------|------|------|------|------|------|------------------------|
| BE0014R | 51.12    | 2.66      | •    | •    |      |      |      |      | •                      |
| CH0002R | 46.81    | 6.94      | •    | •    | •    |      |      | •    |                        |
| CH0004R | 47.05    | 6.98      | •    | •    | •    |      |      |      | •                      |
| CH0005R | 47.07    | 8.46      | •    | •    | •    |      |      |      | •                      |
| CZ0001R | 49.73    | 16.05     | •    | •    | •    |      |      | •    |                        |
| CZ0003R | 49.58    | 15.08     | •    | •    | •    |      | •    | •    |                        |
| DE0001R | 54.93    | 8.31      | •    | •    | •    |      |      | •    |                        |
| DE0002R | 52.80    | 10.76     | •    | •    | •    |      |      | •    |                        |
| DE0003R | 47.91    | 7.91      | •    | •    | •    |      |      |      |                        |
| DE0004R | 49.76    | 7.05      | •    | •    | •    |      |      |      |                        |
| DE0005R | 48.82    | 13.22     | •    | •    | •    |      |      |      |                        |
| DE0007R | 53.17    | 13.03     | •    | •    | •    |      |      | •    |                        |
| DE0008R | 50.65    | 10.77     |      | •    |      |      |      |      |                        |
| DE0009R | 54.43    | 12.73     | •    | •    | •    |      |      |      | •                      |
| DE0044R | 51.53    | 12.93     | •    | •    | •    |      |      |      | •                      |
| DK0003R | 56.35    | 9.60      |      |      |      | •    | •    |      |                        |
| DK0005R | 54.73    | 10.73     | •    |      | •    |      |      |      |                        |
| DK0008R | 56.72    | 11.52     | •    | •    |      | •    | •    |      |                        |
| DK0022R | 56.08    | 9.42      |      | •    | •    |      |      |      | •                      |
| EE0009R | 59.50    | 25.90     | •    | •    |      |      |      |      |                        |
| EE0011R | 58.38    | 21.82     | •    | •    | •    |      |      |      | •                      |
| ES0007R | 37.23    | -3.53     | •    | •    | •    |      |      |      | •                      |
| ES0008R | 43.44    | -4.85     | •    | •    | •    |      |      |      | •                      |
| ES0009R | 41.28    | -3.14     | •    | •    | •    |      |      |      | •                      |
| ES0011R | 38.48    | -6.92     | •    | •    | •    |      |      |      | •                      |
| ES0012R | 39.09    | -1.10     | •    | •    | •    |      |      |      | •                      |
| ES0013R | 41.28    | -5.87     | •    | •    | •    |      |      |      | •                      |
| ES0016R | 43.23    | -7.70     | •    | •    | •    |      |      |      | •                      |
| FI0004R | 62.53    | 24.22     | •    | •    | •    | •    | •    | •    |                        |
| FI0009R | 59.78    | 21.38     |      |      |      | •    | •    |      |                        |
| FI0017R | 60.53    | 27.69     | •    | •    | •    | •    | •    | •    |                        |
| FI0022R | 66.32    | 29.40     | •    | •    | •    | •    | •    | •    |                        |
| FI0037R | 62.58    | 24.18     |      |      |      |      | •    |      |                        |
| FI0053R | 65.00    | 24.69     | •    | •    |      |      |      |      | •                      |
| FR0008R | 48.50    | 7.13      | •    | •    | •    |      |      |      |                        |
| FR0009R | 49.90    | 4.63      | •    | •    | •    |      |      |      |                        |
| FR0010R | 47.27    | 4.08      | •    | •    | •    |      |      |      |                        |
| FR0013R | 43.62    | 0.18      | •    | •    | •    |      |      |      | •                      |
| FR0014R | 47.30    | 6.83      | •    | •    | •    |      |      |      | •                      |
| FR0090R | 48.52    | -4.75     | •    | •    |      |      |      |      | •                      |
| GB0002R | 55.31    | -3.20     | •    | •    | •    |      |      |      |                        |
| GB0006R | 54.44    | -7.87     | •    | •    | •    |      |      |      |                        |
| GB0013R | 50.60    | -3.71     | •    | •    | •    |      |      |      |                        |

| Station | Latitude | Longitude | WNOx | WNHx | WSOx | TNO3 | TNH4 | TSO4 | Extra site (2000-2010) |
|---------|----------|-----------|------|------|------|------|------|------|------------------------|
| GB0014R | 54.33    | -0.81     | •    | •    | •    | •    | •    | •    |                        |
| GB0015R | 57.73    | -4.77     | •    | •    | •    |      |      |      |                        |
| HR0002R | 45.90    | 15.97     | •    | •    | •    |      |      |      |                        |
| HR0004R | 44.82    | 14.98     | •    | •    | •    |      |      |      |                        |
| HU0002R | 46.97    | 19.58     | •    | •    |      | •    | •    |      |                        |
| IE0001R | 51.94    | -10.24    | •    | •    | •    |      |      | •    |                        |
| IT0001R | 42.10    | 12.63     | •    | •    | •    |      |      |      | •                      |
| IT0004R | 45.80    | 8.63      | •    | •    | •    |      |      | •    |                        |
| LT0015R | 55.35    | 21.07     | •    | •    | •    |      | •    | •    |                        |
| LV0010R | 56.16    | 21.17     | •    | •    | •    |      |      | •    |                        |
| NL0009R | 53.33    | 6.28      | •    | •    | •    |      |      |      | •                      |
| NL0091R | 52.30    | 4.50      | •    | •    |      |      |      |      | •                      |
| NO0001R | 58.38    | 8.25      | •    | •    | •    |      | •    | •    |                        |
| NO0002R | 58.39    | 8.25      |      |      |      | •    |      |      |                        |
| NO0015R | 65.83    | 13.92     | •    |      | •    |      |      | •    |                        |
| NO0039R | 62.78    | 8.88      | •    | •    | •    | •    | •    | •    |                        |
| PL0002R | 51.82    | 21.98     | •    | •    | •    | •    | •    |      |                        |
| PL0003R | 50.74    | 15.74     | •    | •    | •    |      | •    | •    |                        |
| PL0004R | 54.75    | 17.53     | •    | •    | •    |      |      |      | •                      |
| PL0005R | 54.15    | 22.07     | •    | •    | •    |      |      |      | •                      |
| RS0005R | 43.40    | 21.95     | •    | •    | •    |      |      |      |                        |
| RU0001R | 68.93    | 28.85     | •    | •    | •    |      |      |      |                        |
| RU0018R | 54.90    | 37.80     | •    | •    |      |      |      |      | •                      |
| SE0002R | 57.42    | 11.93     |      | •    | •    |      |      | •    |                        |
| SE0005R | 63.85    | 15.33     |      |      |      |      | •    |      |                        |
| SE0011R | 56.02    | 13.15     | •    | •    | •    | •    | •    | •    |                        |
| SE0014R | 57.39    | 11.91     | •    |      |      | •    | •    |      |                        |
| SK0004R | 49.15    | 20.28     | •    | •    | •    |      |      |      | •                      |
| SK0006R | 49.05    | 22.27     | •    | •    | •    |      |      |      | •                      |
| SK0007R | 47.96    | 17.86     | •    | •    | •    |      |      |      | •                      |

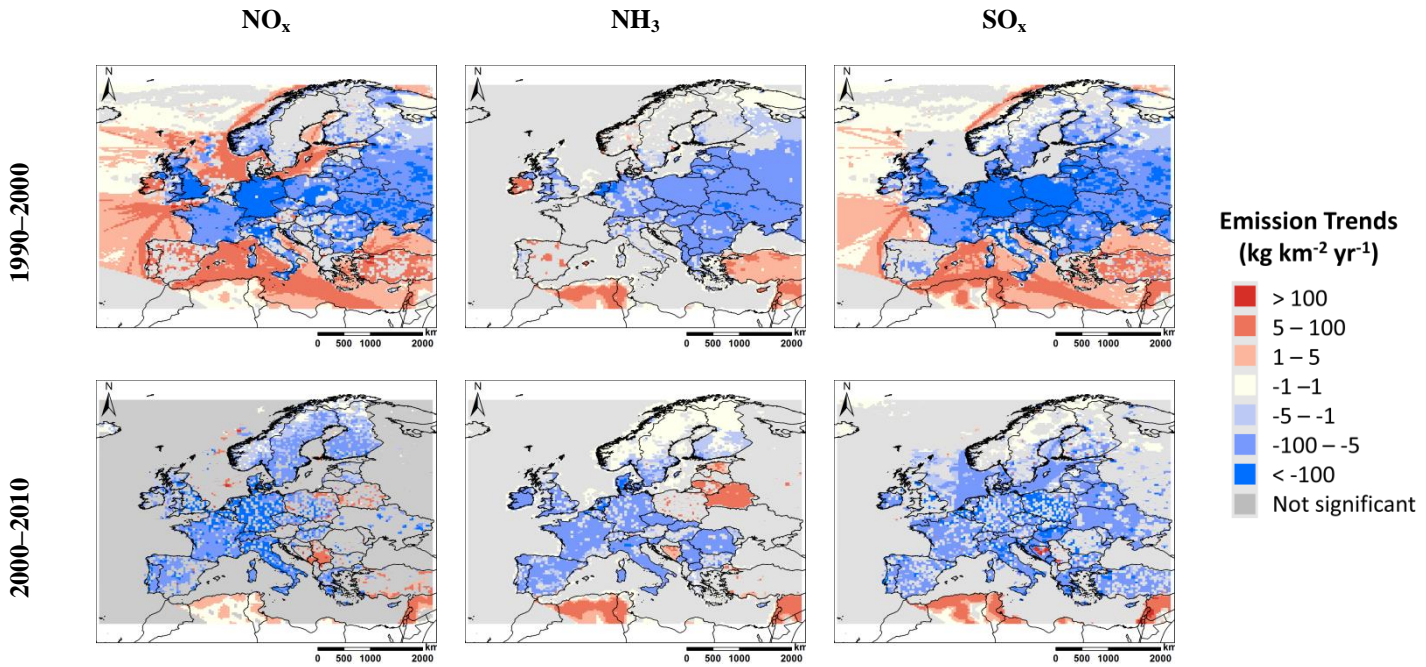


**Figure S3: Maps of the trends (Sen's slopes) in the gridded  $\text{NO}_x$ ,  $\text{NH}_3$  and  $\text{SO}_x$  emissions used in the model simulations for the two ten year periods.**

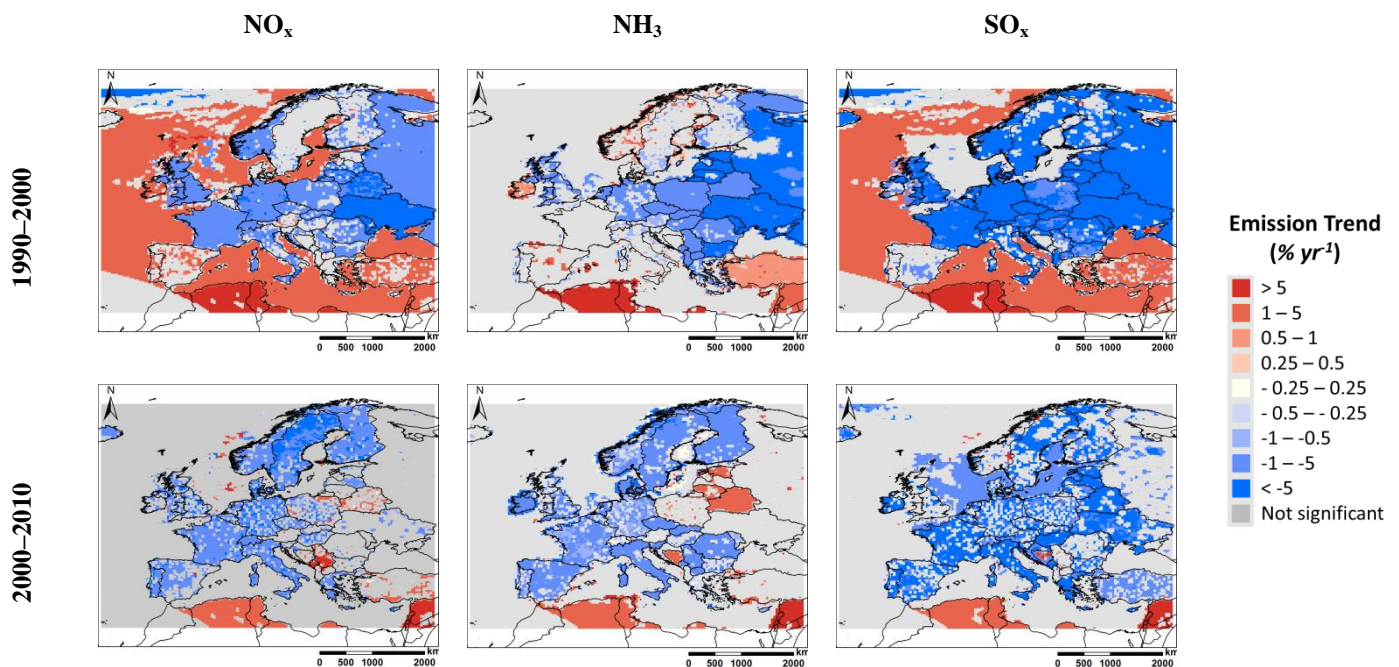


**Figure S4: Maps of the relative trends (trend divided by the estimated emission at the beginning of the period) in the gridded  $\text{NO}_x$ ,  $\text{NH}_3$  and  $\text{SO}_x$  emissions used in the model simulations for the two ten year periods.**

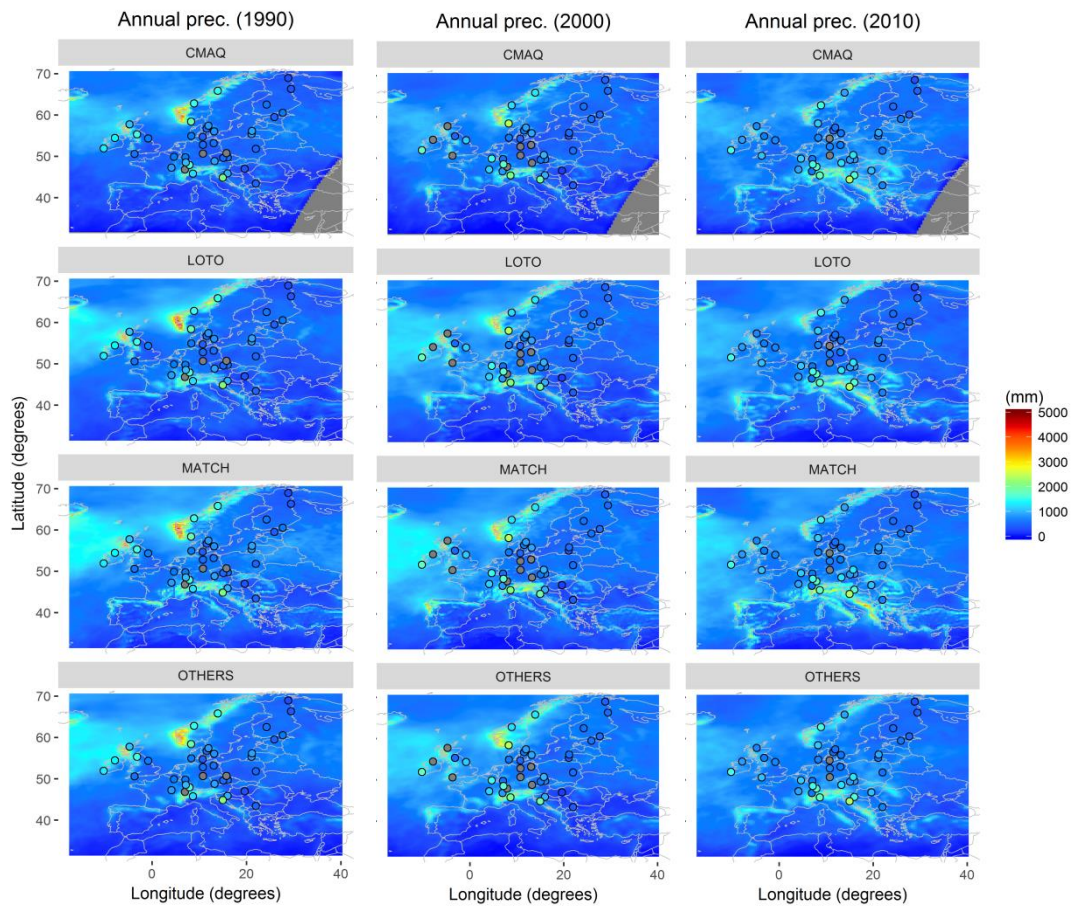


**Figure S5:** Accumulated annual precipitation estimated by the four meteorological models used in the simulations by CMAQ, LOTO, MATCH and the rest of the models (OTHERS) for the years 1990 (left), 2000 (centre) and 2010 (right). The observed precipitation is shown by the coloured circles (grey indicates no data).

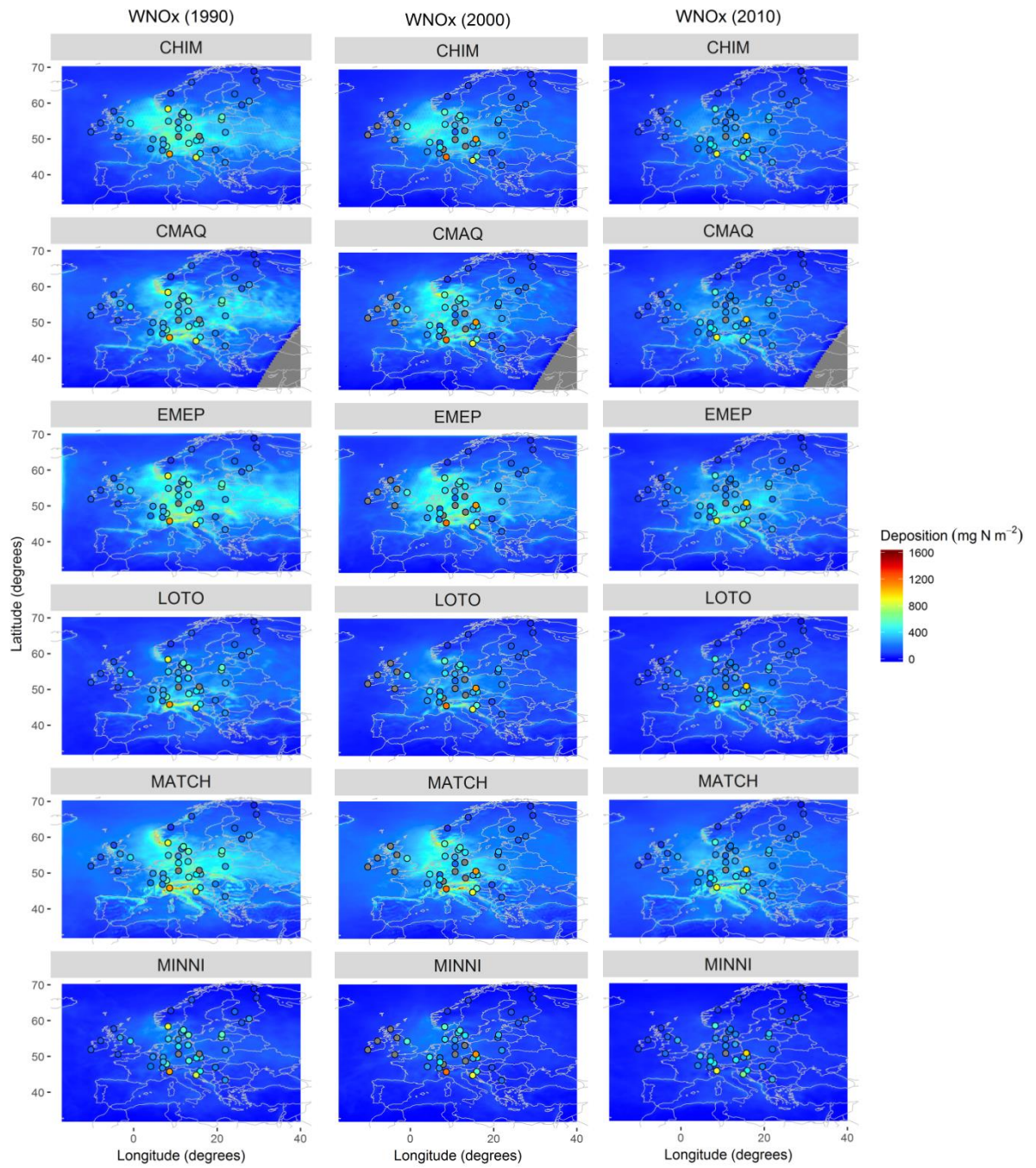


**Figure S6:** Accumulated annual WNOx deposition estimated by the six models for the years 1990 (left), 2000 (centre) and 2010 (right). The observed deposition is shown by the coloured circles (grey indicates no data).

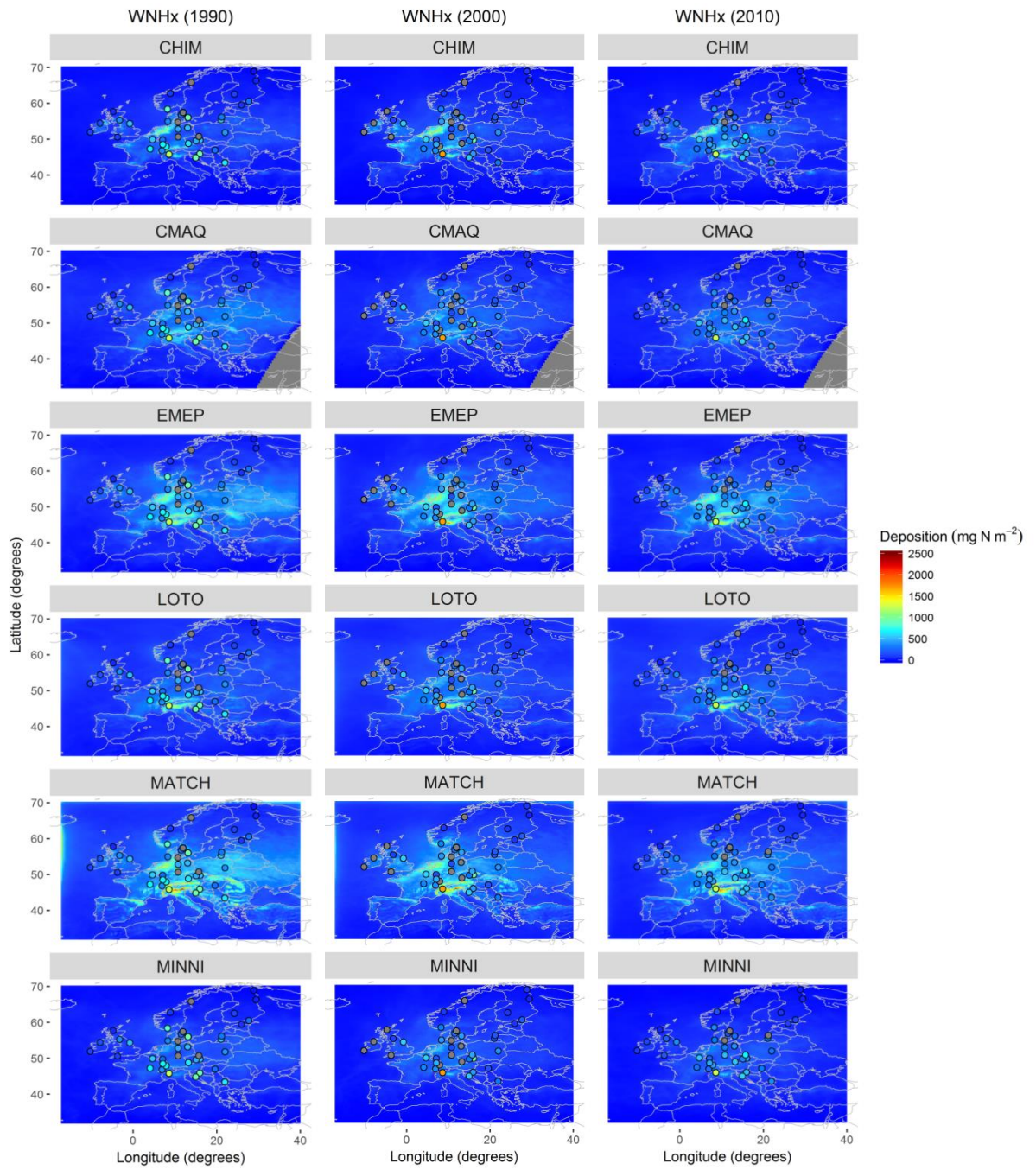


**Figure S7:** Accumulated annual WNHx deposition estimated by the six models for the years 1990 (left), 2000 (centre) and 2010 (right). The observed deposition is shown by the coloured circles (grey indicates no data).

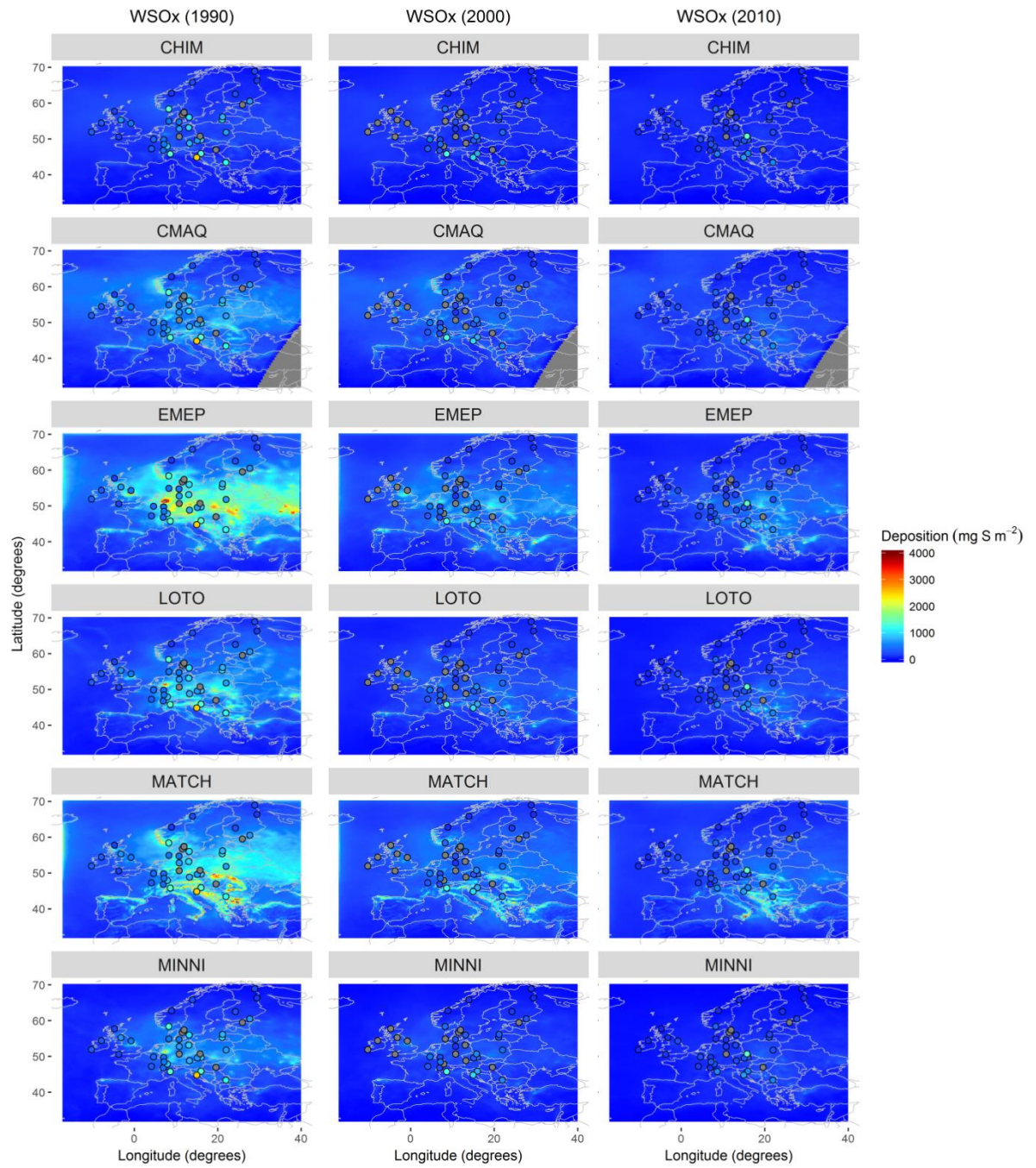


**Figure S8:** Accumulated annual WSOx deposition estimated by the six models for the years 1990 (left) and 2010 (right). The observed deposition is shown by the coloured circles (grey indicates no data).

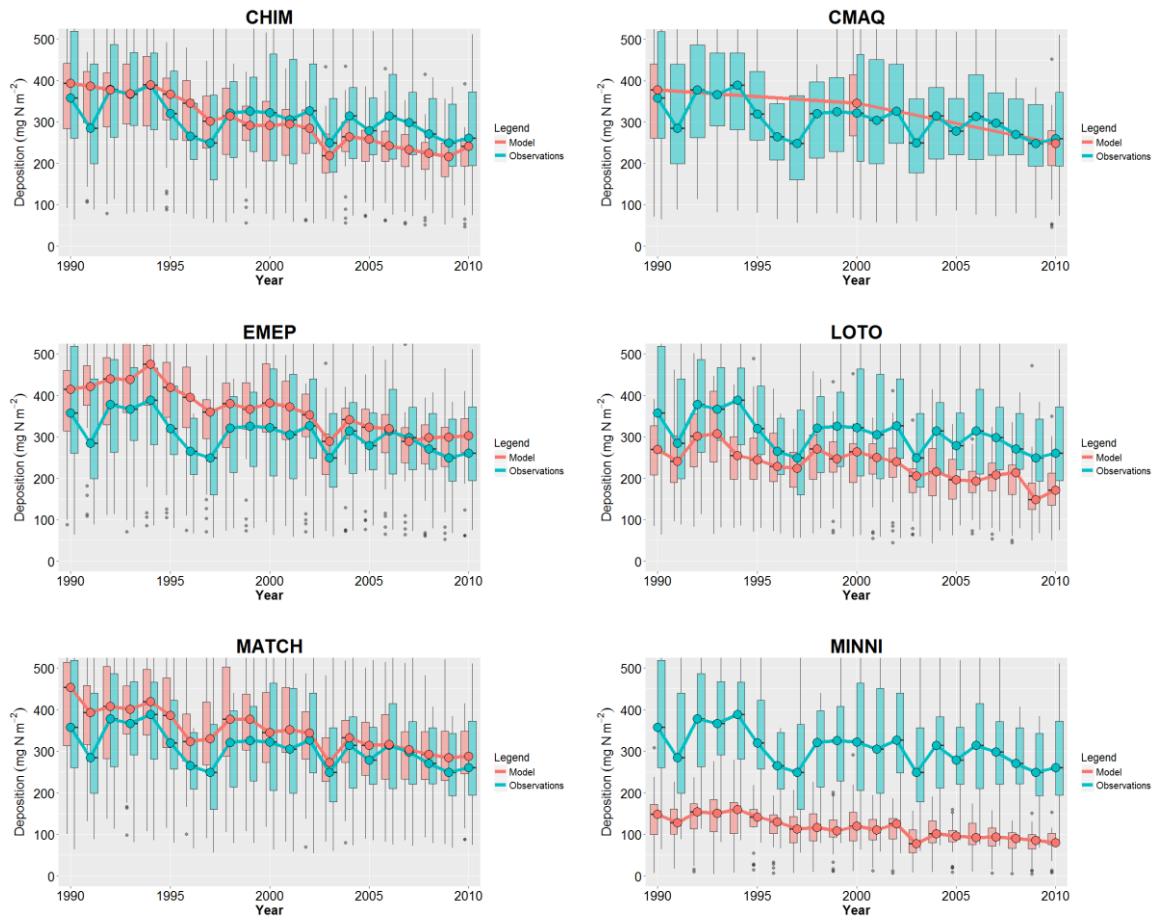


**Figure S9: Tukey-style box plots of the time series of observed and modelled WNOx. Circles represent the annual median value for all measurement sites with a complete 21 year time series.**

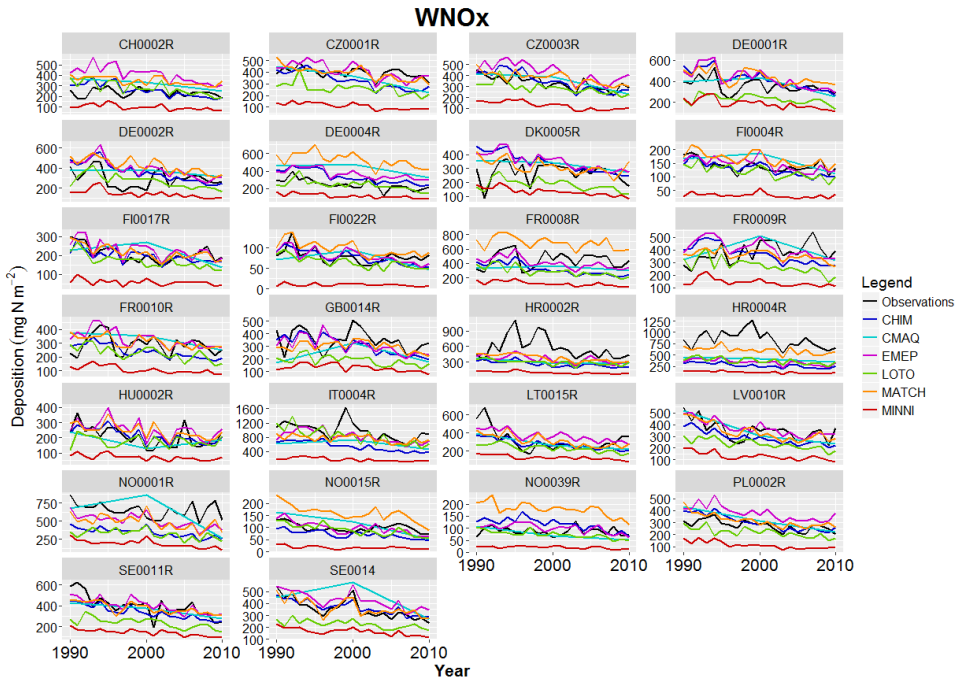


**Figure S10: Time series of observed and modelled WNOx for all measurement sites with a complete 21 year time series.**

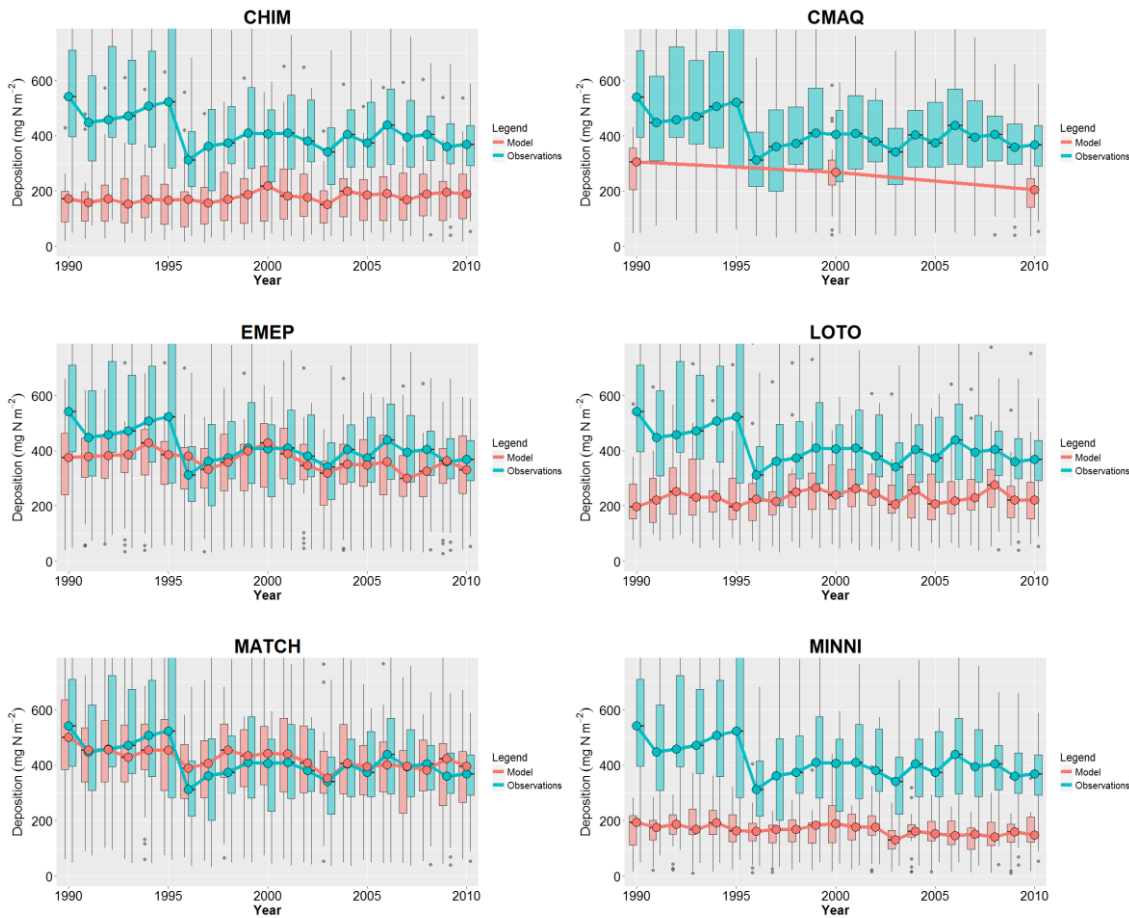


**Figure S11: Tukey-style box plots of the time series of observed and modelled WNHx. Circles represent the annual median value for all measurement sites with a complete 21 year time series.**

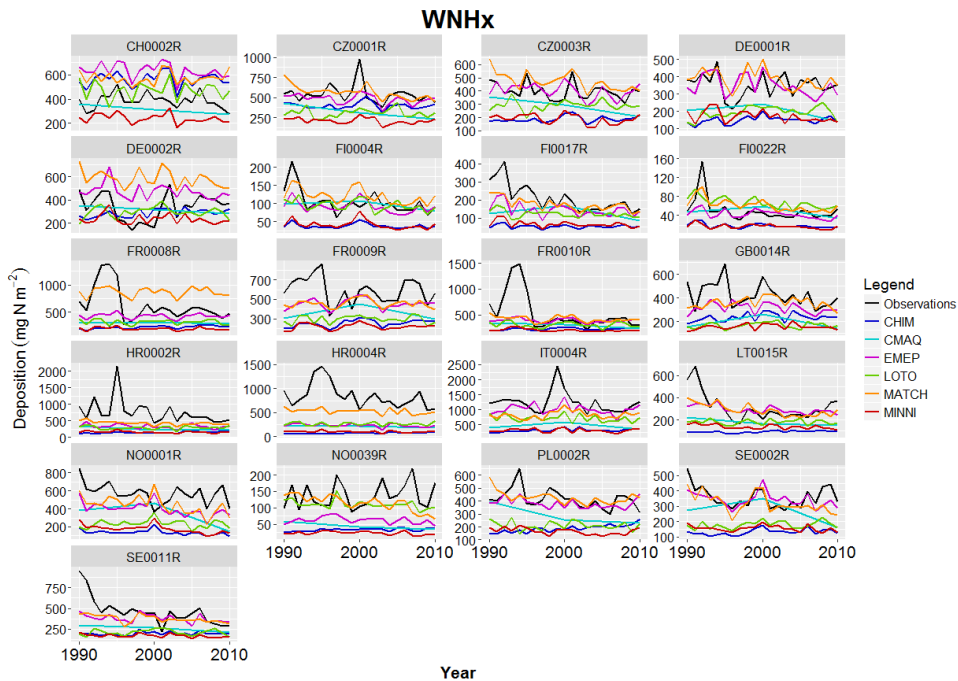


**Figure S12: Time series of observed and modelled WNHx for all measurement sites with a complete 21 year time series.**

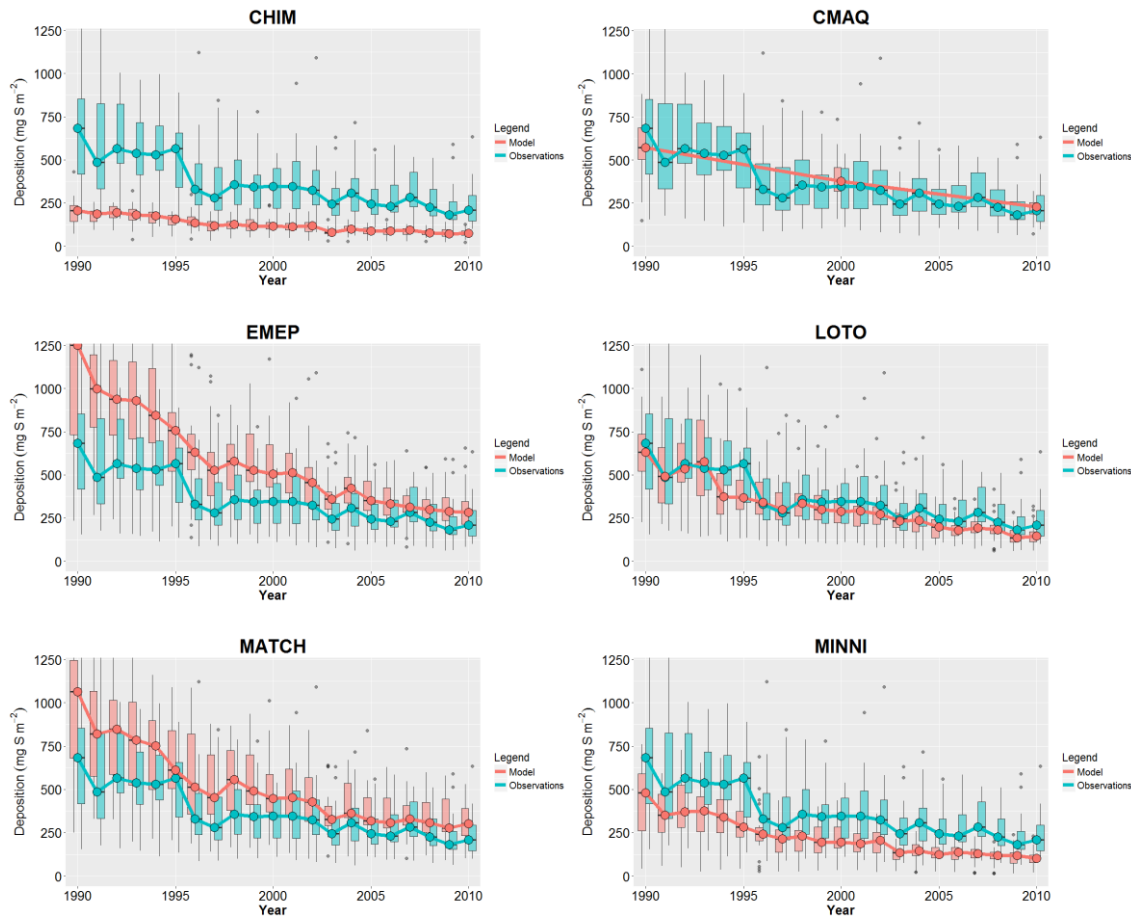


**Figure S13:** Tukey-style box plots of the time series of observed and modelled WSOx. Circles represent the annual median value for all measurement sites with a complete 21 year time series.

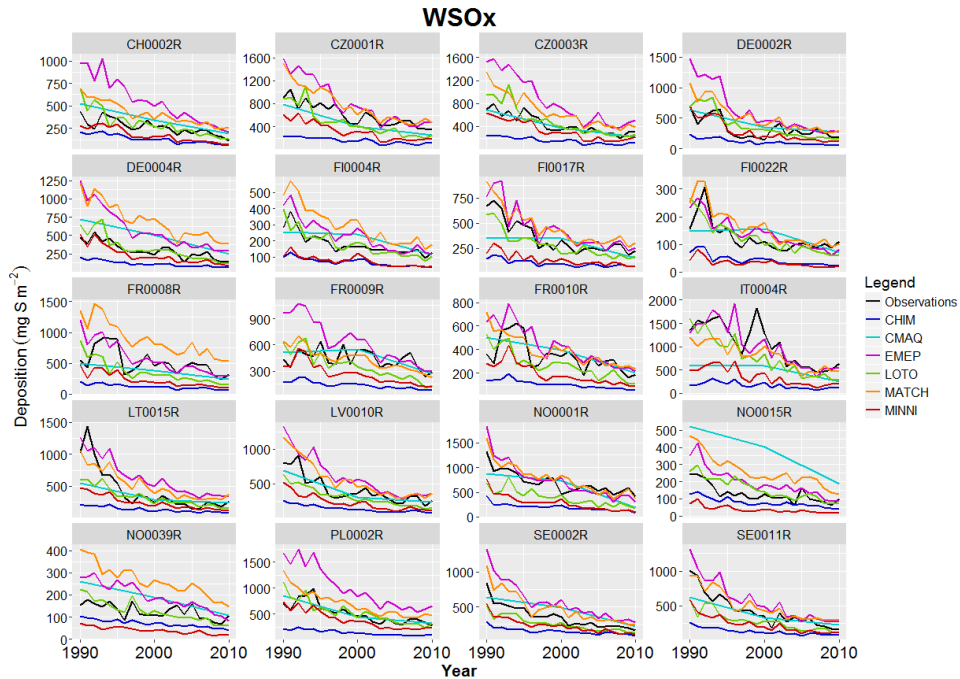


**Figure S14:** Time series of observed and modelled WSOx for all measurement sites with a complete 21 year time series.

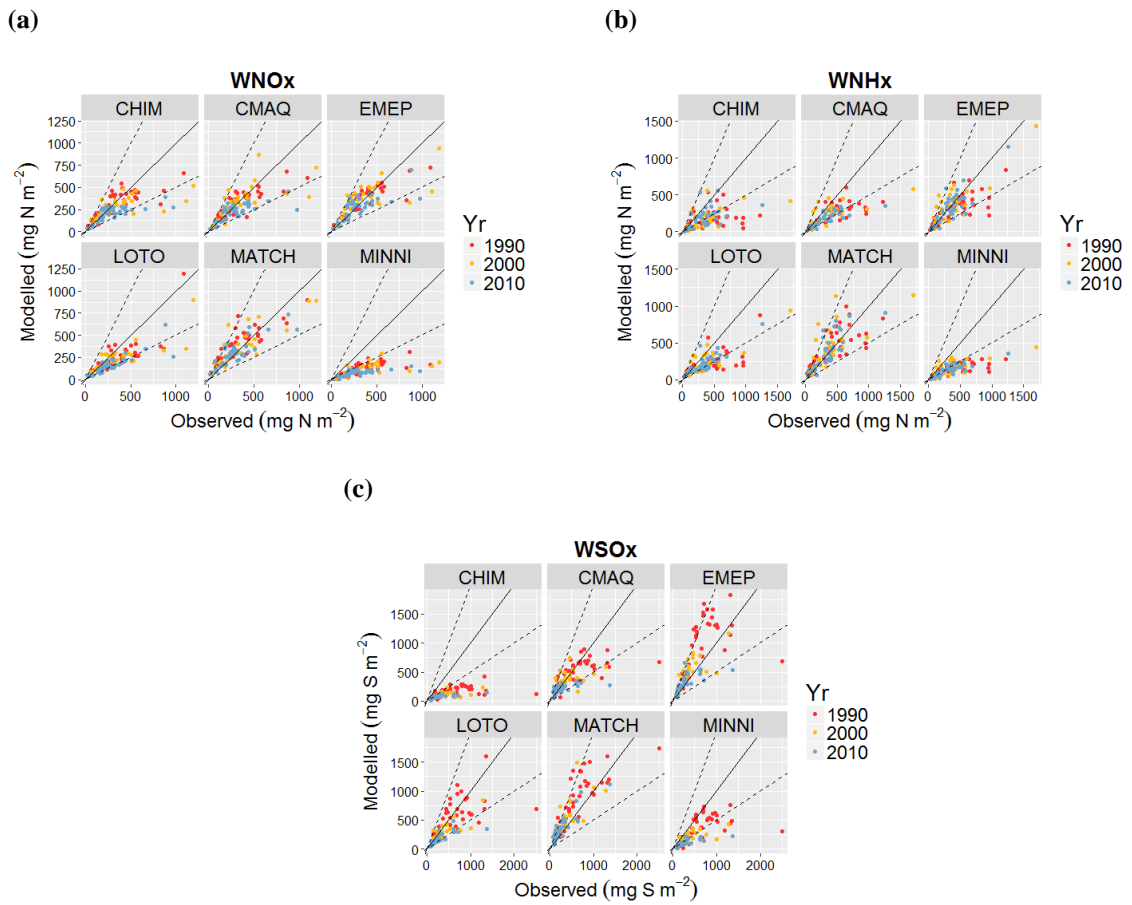


**Figure S15: Modelled vs. observed wet deposition of a) WNOx, b) WNHx and c) WSOx for the years 1990, 2000 and 2010 (colour scale).**

**Table S3: Performance evaluation of the six models that simulated the individual years 1990, 2000 and 2010 and the five models that simulated the full 21 year time series for the three deposition components WNOx, WNHx and WSOx. Values meeting the acceptability criteria of Chang and Hanna (2004) are highlighted in bold green text. FAC2 is the fraction of model predictions within a factor of two of the observations, MG is the geometric mean bias, VG is the geometric variance, FB is the fractional bias, NMSE is the normalised mean squared error and r is the Pearson correlation coefficient.**

|                      |       | 1990, 2000, 2010 |             |             |             |              |             |      | 21 year time series (1990-2010) |             |             |             |              |             |      |
|----------------------|-------|------------------|-------------|-------------|-------------|--------------|-------------|------|---------------------------------|-------------|-------------|-------------|--------------|-------------|------|
| Deposition Component | Model | n                | FAC2        | MG          | VG          | FB           | NMSE        | r    | n                               | FAC2        | MG          | VG          | FB           | NMSE        | r    |
| WNOx                 | CHIM  | 108              | <b>0.87</b> | <b>0.88</b> | <b>1.22</b> | <b>-0.23</b> | <b>0.41</b> | 0.68 | 790                             | <b>0.89</b> | <b>0.87</b> | <b>1.24</b> | <b>-0.23</b> | <b>0.43</b> | 0.63 |
|                      | CMAQ  | 108              | <b>0.93</b> | <b>0.96</b> | <b>1.18</b> | <b>-0.13</b> | <b>0.29</b> | 0.72 | -                               | -           | -           | -           | -            | -           | -    |
|                      | EMEP  | 108              | <b>0.94</b> | <b>1.08</b> | <b>1.16</b> | <b>-0.02</b> | <b>0.21</b> | 0.78 | 790                             | <b>0.90</b> | <b>1.07</b> | <b>1.17</b> | <b>-0.02</b> | <b>0.25</b> | 0.71 |
|                      | LOTO  | 108              | <b>0.77</b> | <b>0.71</b> | <b>1.32</b> | -0.42        | <b>0.48</b> | 0.79 | 790                             | <b>0.82</b> | <b>0.72</b> | <b>1.29</b> | -0.39        | <b>0.48</b> | 0.76 |
|                      | MATCH | 108              | <b>0.89</b> | <b>1.20</b> | <b>1.22</b> | <b>0.06</b>  | <b>0.15</b> | 0.84 | 790                             | <b>0.88</b> | <b>1.18</b> | <b>1.21</b> | <b>0.06</b>  | <b>0.17</b> | 0.81 |
|                      | MINNI | 108              | 0.16        | 0.30        | 5.18        | -1.05        | 2.71        | 0.65 | 790                             | 0.16        | 0.30        | 5.45        | -1.06        | 2.81        | 0.59 |
| WNHx                 | CHIM  | 103              | 0.41        | 0.45        | <b>2.94</b> | -0.73        | <b>1.49</b> | 0.45 | 758                             | 0.41        | 0.45        | <b>3.02</b> | -0.74        | 1.64        | 0.35 |
|                      | CMAQ  | 103              | <b>0.68</b> | 0.63        | <b>1.56</b> | -0.54        | <b>0.84</b> | 0.68 | -                               | -           | -           | -           | -            | -           | -    |
|                      | EMEP  | 103              | <b>0.83</b> | <b>0.89</b> | <b>1.27</b> | <b>-0.15</b> | <b>0.25</b> | 0.78 | 758                             | <b>0.82</b> | <b>0.88</b> | <b>1.30</b> | <b>-0.18</b> | <b>0.38</b> | 0.66 |
|                      | LOTO  | 103              | <b>0.67</b> | 0.66        | <b>1.59</b> | -0.52        | <b>0.71</b> | 0.75 | 758                             | <b>0.68</b> | 0.67        | <b>1.54</b> | -0.52        | <b>0.82</b> | 0.67 |
|                      | MATCH | 103              | <b>0.86</b> | <b>1.13</b> | <b>1.26</b> | <b>0.05</b>  | <b>0.25</b> | 0.72 | 758                             | <b>0.87</b> | <b>1.13</b> | <b>1.26</b> | <b>0.04</b>  | <b>0.30</b> | 0.66 |
|                      | MINNI | 103              | 0.34        | 0.40        | <b>2.96</b> | -0.88        | 1.82        | 0.72 | 758                             | 0.30        | 0.39        | <b>3.22</b> | -0.92        | 2.10        | 0.63 |
| WSOx                 | CHIM  | 97               | 0.23        | 0.32        | 4.82        | -1.12        | 3.96        | 0.55 | 724                             | 0.20        | 0.32        | 4.85        | -1.13        | 3.78        | 0.55 |
|                      | CMAQ  | 97               | <b>0.77</b> | <b>0.95</b> | <b>1.35</b> | <b>-0.20</b> | <b>0.57</b> | 0.64 | -                               | -           | -           | -           | -            | -           | -    |
|                      | EMEP  | 97               | <b>0.76</b> | 1.34        | <b>1.31</b> | <b>0.27</b>  | <b>0.51</b> | 0.65 | 724                             | <b>0.83</b> | 1.31        | <b>1.29</b> | <b>0.22</b>  | <b>0.38</b> | 0.67 |
|                      | LOTO  | 97               | <b>0.86</b> | <b>0.77</b> | <b>1.27</b> | <b>-0.26</b> | <b>0.54</b> | 0.70 | 724                             | <b>0.85</b> | <b>0.76</b> | <b>1.28</b> | -0.32        | <b>0.51</b> | 0.74 |
|                      | MATCH | 97               | <b>0.85</b> | 1.41        | <b>1.28</b> | <b>0.26</b>  | <b>0.27</b> | 0.83 | 724                             | <b>0.86</b> | 1.35        | <b>1.25</b> | <b>0.22</b>  | <b>0.22</b> | 0.83 |
|                      | MINNI | 97               | <b>0.51</b> | 0.47        | <b>2.42</b> | -0.65        | <b>1.33</b> | 0.64 | 724                             | 0.48        | 0.46        | <b>2.47</b> | -0.70        | <b>1.39</b> | 0.64 |

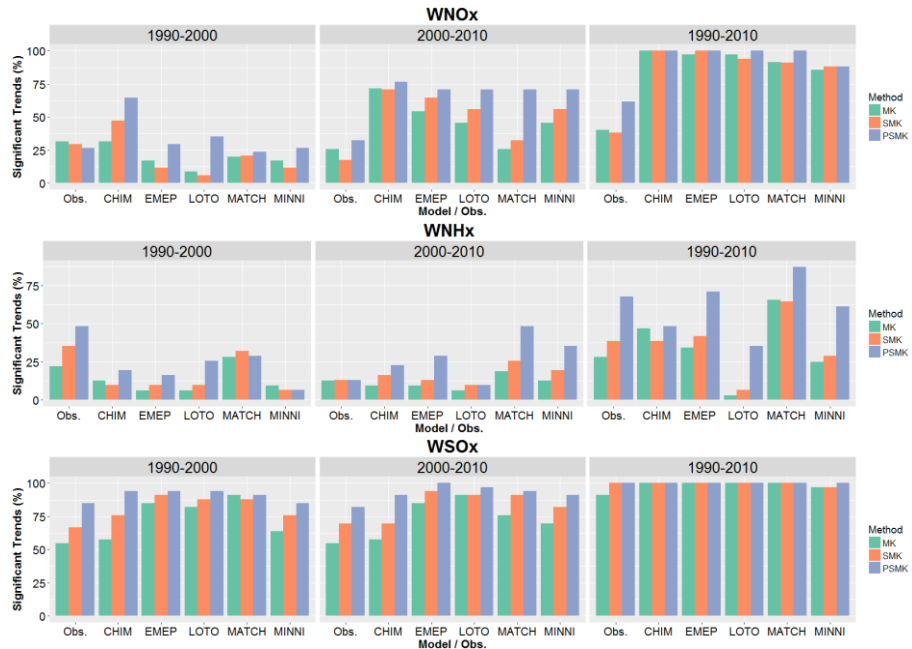


**Figure S16:** Proportion of observed/modelled trends that are significant for each trend estimation method (MK: Mann-Kendall; SMK: Seasonal Mann-Kendall; PSMK: Partial Seasonal Mann-Kendall) for WNOx (top), WNHx (middle) and WSOx (bottom) for the two 10 year periods and the full 20 year period.

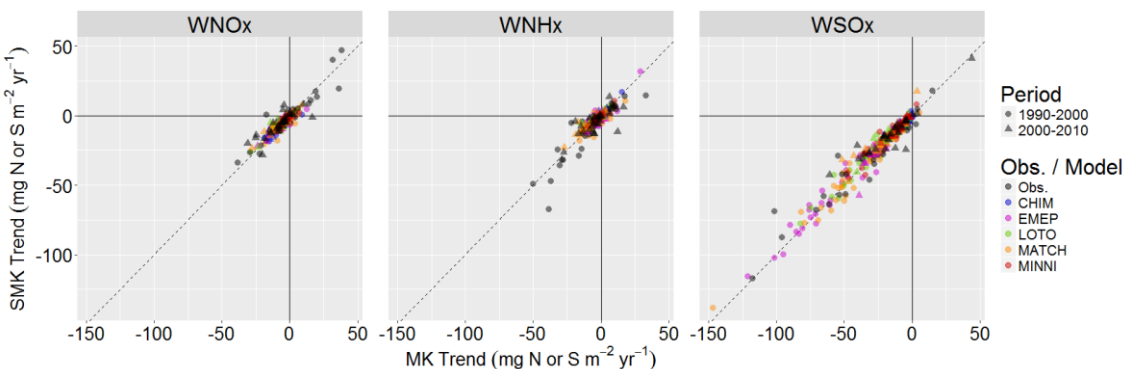


**Figure S17:** Observed/modelled absolute trends of WNOx, WNHx and WSOx calculated using the Seasonal Mann-Kendall (SMK) method versus those calculated using the Mann-Kendall (MK) method for the different time periods (symbols). The dashed line is the 1:1 line.

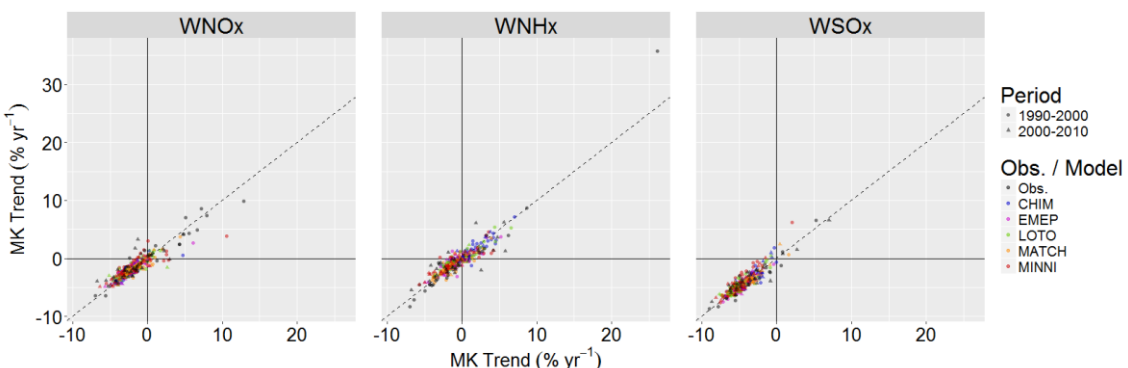


**Figure S18:** Observed/modelled relative trends of WNOx, WNHx and WSOx calculated using the Seasonal Mann-Kendall (SMK) method versus those calculated using the Mann-Kendall (MK) method for the different time periods (symbols). The dashed line is the 1:1 line.

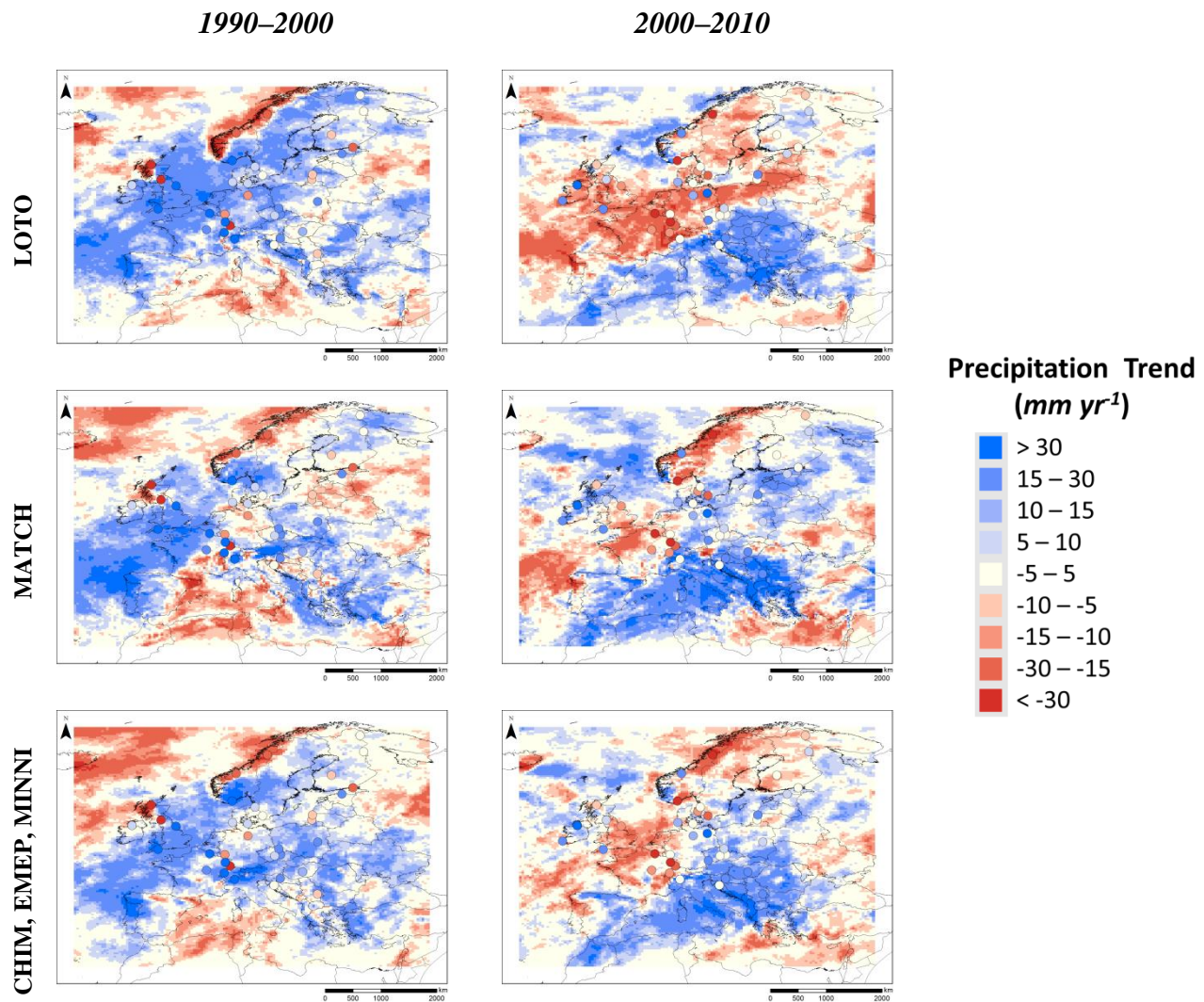


**Figure S19:** Maps of modelled (coloured field) and observed (circles) precipitation trends for the periods 1990-2000 and 2000–2010.

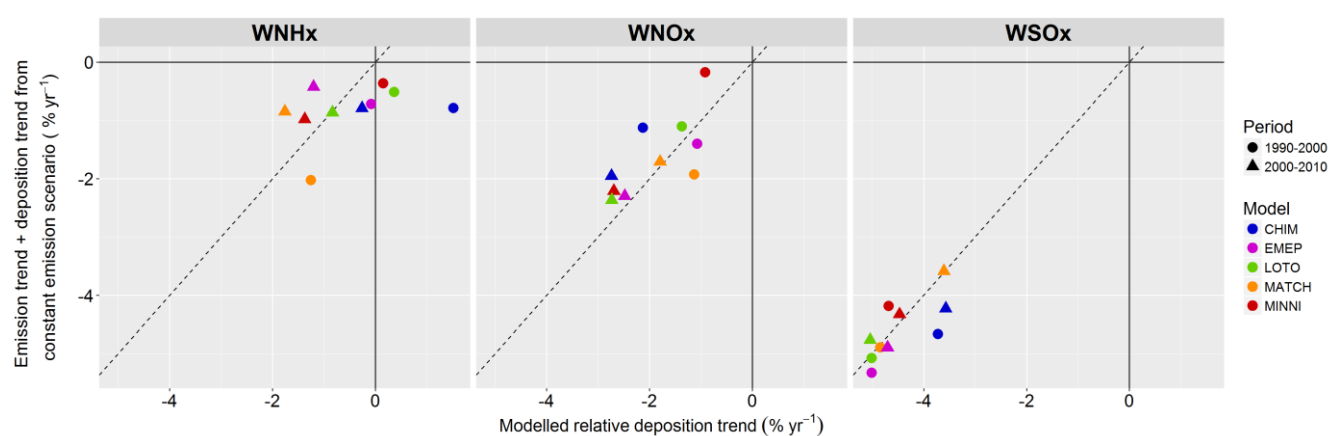


**Figure S20:** Scatter plots showing the sum of the median domain emission trends and the median wet deposition trends for the simulations with constant emissions vs. the median wet deposition trends for the simulations with changing emissions.

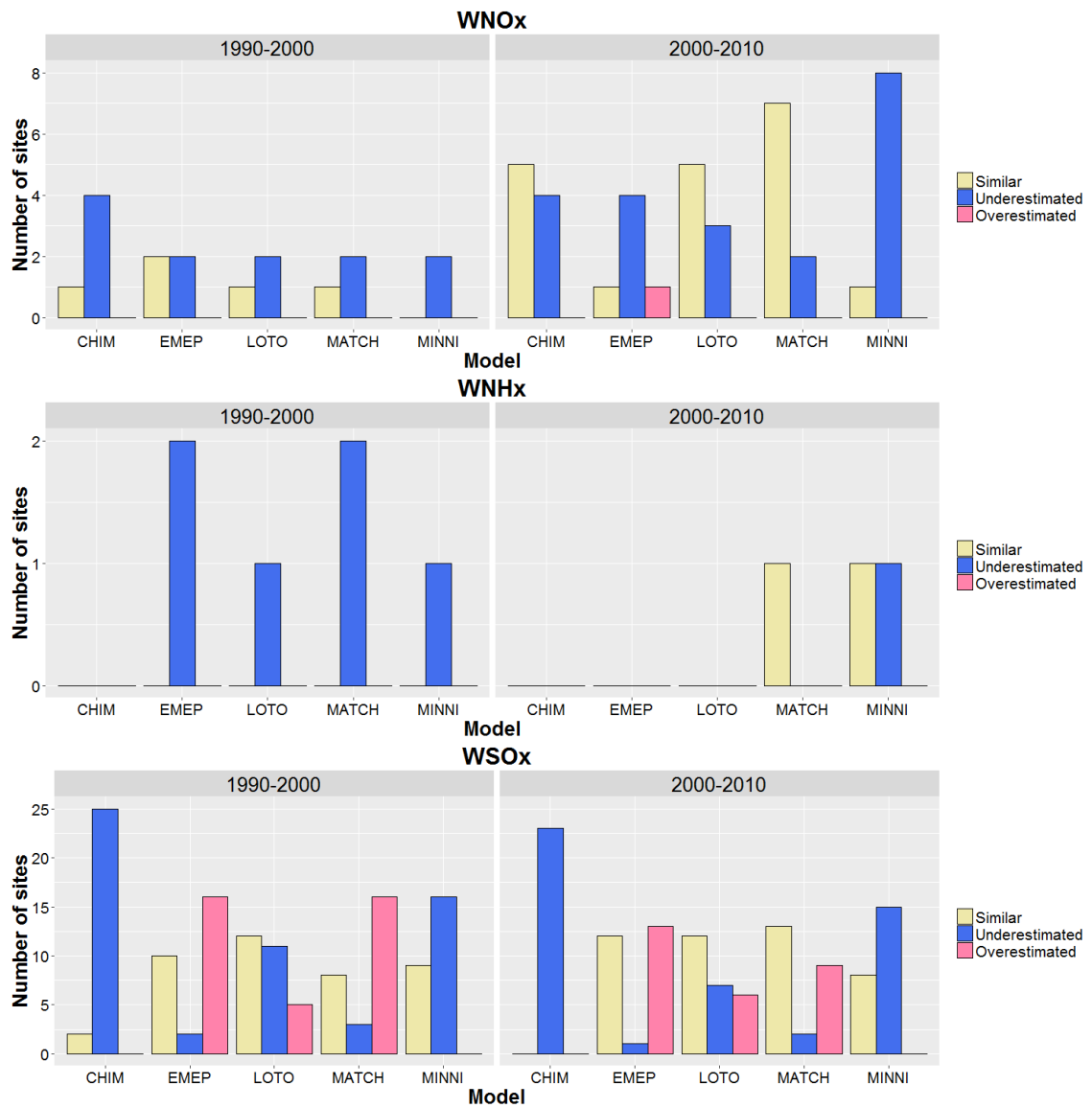


**Figure S21:** Number of sites for which the five models estimated statistically similar trends to those observed (i.e. have overlapping 95% confidence intervals) or underestimated or overestimated the observed trends. Only sites with significant ( $p < 0.05$ ) observed and modelled trends are shown.

**Table S4: Performance evaluation of the absolute and relative trends of WSOx for the two ten year periods. Values meeting the acceptability criteria of Chang and Hanna (2004) are highlighted in bold green text. FAC2 is the fraction of model predictions within a factor of two of the observations, FB is the fractional bias, NMSE is the normalised mean squared error and r is the Pearson correlation coefficient.**

| Trend               | Model | n  | Absolute Trends |              |             | Relative Trends |             |              |             |      |
|---------------------|-------|----|-----------------|--------------|-------------|-----------------|-------------|--------------|-------------|------|
|                     |       |    | FAC2            | FB           | NMSE        | r               | FAC2        | FB           | NMSE        | r    |
| WSOx<br>(1990-2000) | CHIM  | 33 | 0.12            | -1.28        | 5.84        | 0.56            | <b>0.79</b> | <b>-0.15</b> | <b>0.33</b> | 0.65 |
|                     | EMEP  | 33 | <b>0.61</b>     | 0.47         | <b>0.66</b> | 0.58            | <b>0.88</b> | <b>0.17</b>  | <b>0.25</b> | 0.70 |
|                     | LOTO  | 33 | <b>0.61</b>     | <b>-0.10</b> | <b>0.72</b> | 0.46            | <b>0.82</b> | <b>0.13</b>  | <b>0.29</b> | 0.56 |
|                     | MATCH | 33 | <b>0.73</b>     | <b>0.29</b>  | <b>0.33</b> | 0.78            | <b>0.82</b> | <b>0.07</b>  | <b>0.24</b> | 0.70 |
|                     | MINNI | 33 | 0.33            | -0.59        | <b>1.39</b> | 0.53            | <b>0.76</b> | <b>-0.04</b> | <b>0.31</b> | 0.64 |
| WSOx<br>(2000-2010) | CHIM  | 33 | 0.15            | -1.14        | 5.54        | 0.28            | <b>0.73</b> | <b>-0.04</b> | <b>0.66</b> | 0.13 |
|                     | EMEP  | 33 | <b>0.55</b>     | 0.43         | <b>0.83</b> | 0.41            | <b>0.88</b> | <b>0.28</b>  | <b>0.46</b> | 0.29 |
|                     | LOTO  | 33 | <b>0.67</b>     | <b>-0.06</b> | <b>1.14</b> | 0.26            | <b>0.79</b> | 0.31         | <b>0.44</b> | 0.37 |
|                     | MATCH | 33 | <b>0.73</b>     | <b>0.16</b>  | <b>1.49</b> | -0.02           | <b>0.88</b> | <b>-0.01</b> | <b>0.49</b> | 0.35 |
|                     | MINNI | 33 | 0.45            | -0.56        | 2.00        | 0.35            | <b>0.79</b> | <b>0.25</b>  | <b>0.47</b> | 0.32 |

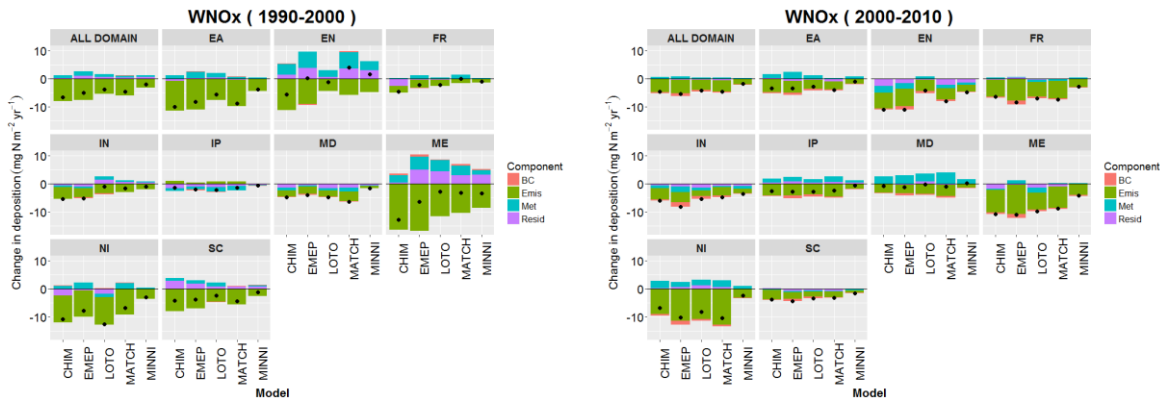


**Figure S22: The mean contributions of the different factors (Bars) (BC: Boundary conditions; Emis: Emissions; Met: Meteorology and Resid: Residual interactions) to the WNOx trends (black circles) for all land grid cells for the entire domain and each subregion for the five models and two time periods.**

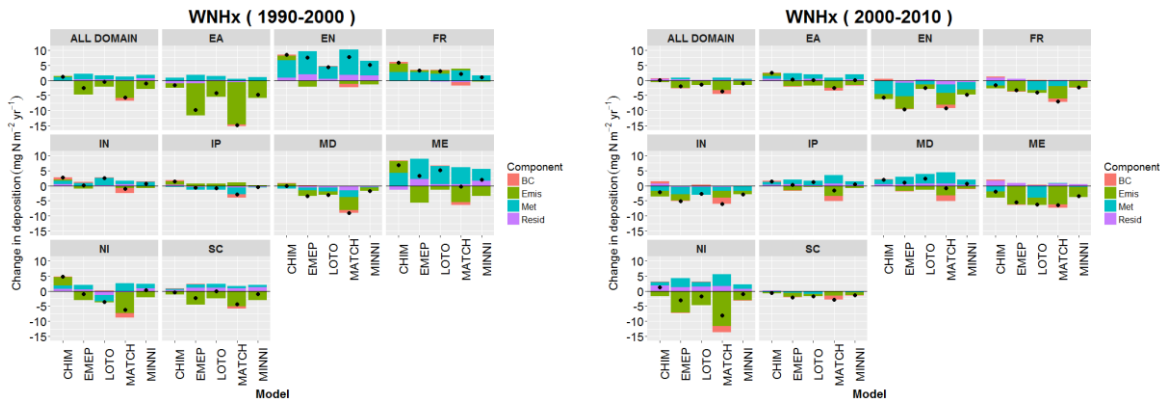


**Figure S23: The mean contributions of the different factors (Bars) (BC: Boundary conditions; Emis: Emissions; Met: Meteorology and Resid: Residual interactions) to the WNHx trends (black circles) for all land grid cells for the entire domain and each subregion for the five models and two time periods.**

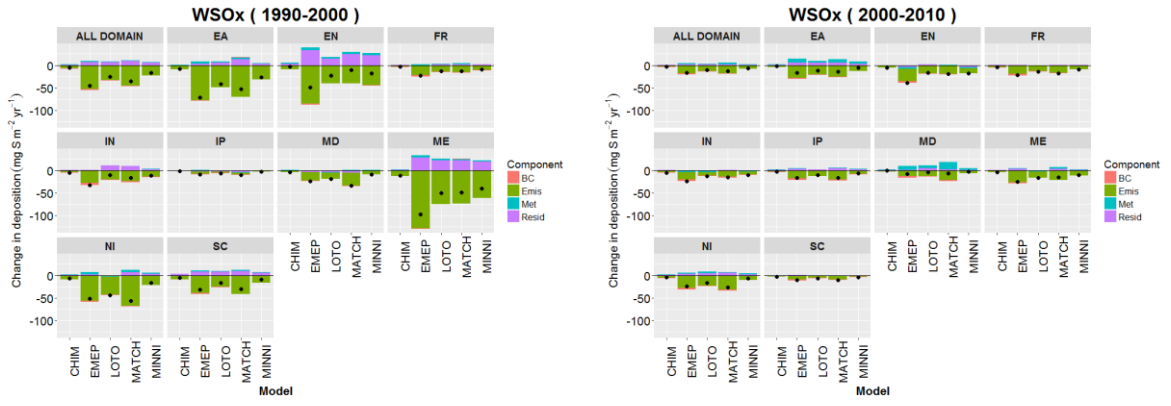
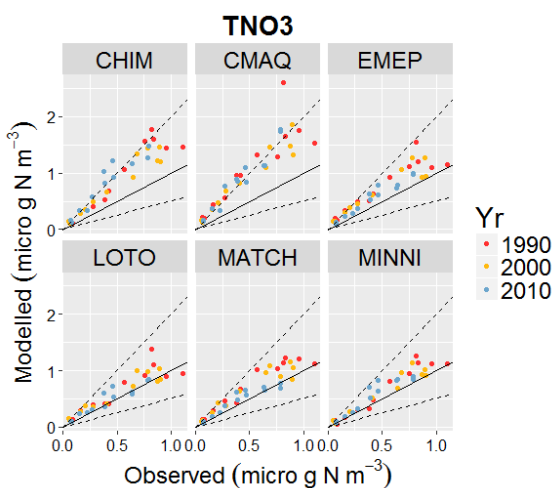


**Figure S24:** The mean contributions of the different factors (Bars) (BC: Boundary conditions; Emis: Emissions; Met: Meteorology and Resid: Residual interactions) to the WSOx trends (black circles) for all land grid cells for the entire domain and each subregion for the five models and two time periods.

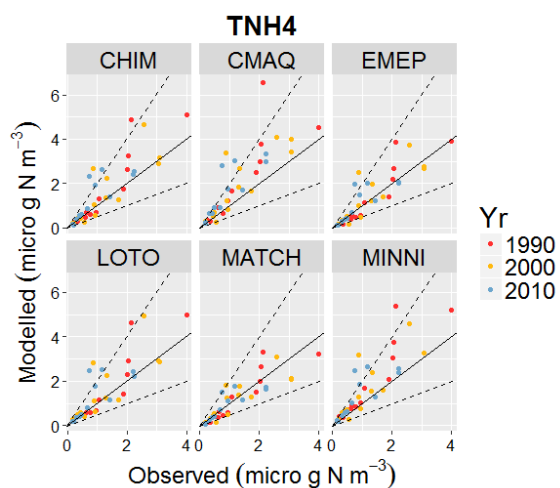
**Table S5:** Performance evaluation of the seasonal and annual accumulated precipitation (at the wet deposition sites) used in the simulations of the six models that simulated the individual years 1990, 2000 and 2010 and the five models that simulated the full 21 year time series. Values meeting the acceptability criteria of Chang and Hanna (2004) are highlighted in bold green text. FAC2 is the fraction of model predictions within a factor of two of the observations, MG is the geometric mean bias, VG is the geometric variance, FB is the fractional bias, NMSE is the normalised mean squared error and r is the Pearson correlation coefficient.

| Season | Model  | 1990, 2000, 2010 |             |             |             |       |             |      | 21 year time series (1990-2010) |             |             |             |       |             |      |
|--------|--------|------------------|-------------|-------------|-------------|-------|-------------|------|---------------------------------|-------------|-------------|-------------|-------|-------------|------|
|        |        | n                | FAC2        | MG          | VG          | FB    | NMSE        | r    | n                               | FAC2        | MG          | VG          | FB    | NMSE        | r    |
| Winter | CMAQ   | 108              | <b>0.92</b> | <b>1.07</b> | <b>1.24</b> | -0.02 | <b>0.21</b> | 0.77 | -                               | -           | -           | -           | -     | -           | -    |
|        | LOTO   | 108              | <b>0.92</b> | <b>1.06</b> | <b>1.23</b> | 0.00  | <b>0.21</b> | 0.77 | 775                             | <b>0.75</b> | <b>1.04</b> | <b>1.45</b> | -0.01 | <b>0.41</b> | 0.53 |
|        | MATCH  | 108              | <b>0.94</b> | <b>1.11</b> | <b>1.20</b> | 0.03  | <b>0.17</b> | 0.81 | 775                             | <b>0.79</b> | <b>1.07</b> | <b>1.39</b> | 0.00  | <b>0.35</b> | 0.58 |
|        | OTHERS | 108              | <b>0.90</b> | <b>1.09</b> | <b>1.29</b> | 0.01  | <b>0.24</b> | 0.72 | 775                             | <b>0.75</b> | <b>1.09</b> | <b>1.45</b> | 0.00  | <b>0.43</b> | 0.47 |
| Spring | CMAQ   | 110              | <b>0.89</b> | <b>0.93</b> | <b>1.26</b> | -0.11 | <b>0.25</b> | 0.67 | -                               | -           | -           | -           | -     | -           | -    |
|        | LOTO   | 110              | <b>0.88</b> | <b>0.99</b> | <b>1.23</b> | -0.03 | <b>0.17</b> | 0.76 | 783                             | <b>0.82</b> | <b>1.04</b> | <b>1.36</b> | -0.02 | <b>0.36</b> | 0.50 |
|        | MATCH  | 110              | <b>0.94</b> | <b>1.11</b> | <b>1.21</b> | 0.03  | <b>0.14</b> | 0.77 | 783                             | <b>0.82</b> | <b>1.04</b> | <b>1.35</b> | -0.03 | <b>0.35</b> | 0.51 |
|        | OTHERS | 110              | <b>0.89</b> | <b>1.04</b> | <b>1.28</b> | -0.03 | <b>0.26</b> | 0.60 | 783                             | <b>0.79</b> | <b>1.01</b> | <b>1.41</b> | -0.07 | <b>0.44</b> | 0.36 |
| Summer | CMAQ   | 110              | <b>0.86</b> | <b>0.80</b> | <b>1.22</b> | -0.21 | <b>0.19</b> | 0.67 | -                               | -           | -           | -           | -     | -           | -    |
|        | LOTO   | 110              | <b>0.75</b> | <b>0.72</b> | <b>1.50</b> | -0.30 | <b>0.34</b> | 0.46 | 776                             | <b>0.75</b> | <b>0.90</b> | <b>1.48</b> | -0.10 | <b>0.34</b> | 0.20 |
|        | MATCH  | 110              | <b>0.92</b> | <b>1.02</b> | <b>1.16</b> | 0.01  | <b>0.16</b> | 0.62 | 776                             | <b>0.78</b> | <b>1.01</b> | <b>1.39</b> | 0.00  | <b>0.29</b> | 0.27 |
|        | OTHERS | 110              | <b>0.83</b> | <b>0.82</b> | <b>1.45</b> | -0.16 | <b>0.26</b> | 0.49 | 776                             | <b>0.72</b> | <b>0.80</b> | <b>1.67</b> | -0.20 | <b>0.44</b> | 0.08 |
| Autumn | CMAQ   | 109              | <b>0.89</b> | <b>0.89</b> | <b>1.19</b> | -0.22 | <b>0.33</b> | 0.80 | -                               | -           | -           | -           | -     | -           | -    |
|        | LOTO   | 109              | <b>0.92</b> | <b>0.97</b> | <b>1.18</b> | -0.12 | <b>0.22</b> | 0.81 | 773                             | <b>0.82</b> | <b>0.94</b> | <b>1.41</b> | -0.08 | <b>0.35</b> | 0.51 |
|        | MATCH  | 109              | <b>0.96</b> | <b>0.98</b> | <b>1.14</b> | -0.10 | <b>0.18</b> | 0.85 | 773                             | <b>0.84</b> | <b>0.93</b> | <b>1.31</b> | -0.11 | <b>0.33</b> | 0.56 |
|        | OTHERS | 109              | <b>0.84</b> | <b>0.91</b> | <b>1.23</b> | -0.19 | <b>0.33</b> | 0.75 | 773                             | <b>0.79</b> | <b>0.89</b> | <b>1.39</b> | -0.16 | <b>0.44</b> | 0.42 |
| Annual | CMAQ   | 437              | <b>0.89</b> | <b>0.92</b> | <b>1.23</b> | -0.15 | <b>0.25</b> | 0.74 | -                               | -           | -           | -           | -     | -           | -    |
|        | LOTO   | 437              | <b>0.87</b> | <b>0.92</b> | <b>1.28</b> | -0.11 | <b>0.24</b> | 0.74 | 3868                            | <b>0.81</b> | <b>0.98</b> | <b>1.36</b> | -0.06 | <b>0.32</b> | 0.84 |
|        | MATCH  | 437              | <b>0.94</b> | <b>1.05</b> | <b>1.17</b> | -0.01 | <b>0.17</b> | 0.79 | 3868                            | <b>0.84</b> | <b>1.01</b> | <b>1.31</b> | -0.04 | <b>0.29</b> | 0.85 |
|        | OTHERS | 437              | <b>0.86</b> | <b>0.96</b> | <b>1.31</b> | -0.10 | <b>0.28</b> | 0.67 | 3868                            | <b>0.79</b> | <b>0.94</b> | <b>1.42</b> | -0.11 | <b>0.45</b> | 0.78 |

(a)



(b)



(c)

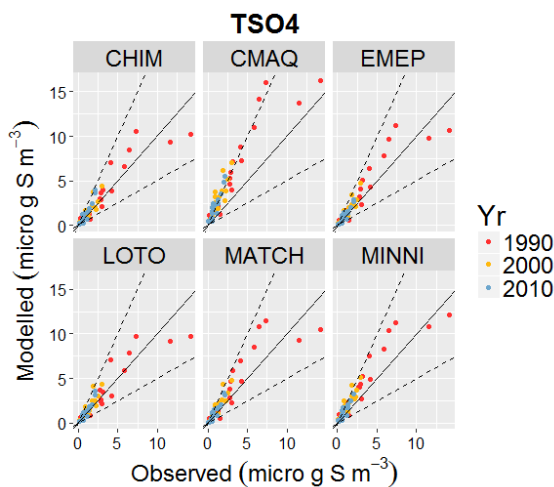


**Figure S25: Modelled vs. observed mean annual concentrations of a) TNO3, b) TNH4 and c) TSO4 for the years 1990, 2000 and 2010 (colour scale).**

**Table S6: Performance evaluation of the six models that simulated the individual years 1990, 2000 and 2010 for the three atmospheric components TNO3, TNH4 and TSO4 at all sites and only at sites with wet deposition observations. Values meeting the acceptability criteria of Chang and Hanna (2004) are highlighted in bold green text. FAC2 is the fraction of model predictions within a factor of two of the observations, MG is the geometric mean bias, VG is the geometric variance, FB is the fractional bias, NMSE is the normalised mean squared error and r is the Pearson correlation coefficient.**

| Atmospheric concentrations<br>1990, 2000, 2010 |       |    |             |             |             |             |             |      |                      | Wet deposition at concentration sites<br>1990, 2000, 2010 |             |             |             |             |             |      |
|--|-------|----|-------------|-------------|-------------|-------------|-------------|------|----------------------|---|-------------|-------------|-------------|-------------|-------------|------|
| Concentration Component                        | Model | n  | FAC2        | MG          | VG          | FB          | NMSE        | r    | Deposition Component | n   | FAC2        | MG          | VG          | FB          | NMSE        | r    |
| TNO3   | CHIM  | 37 | <b>0.73</b> | 1.81        | <b>1.48</b> | 0.56        | <b>0.49</b> | 0.94 | WNOx                 | 30  | <b>0.97</b> | <b>0.98</b> | <b>1.10</b> | -0.07       | <b>0.09</b> | 0.89 |
|  | CMAQ  | 37 | 0.30        | 2.15        | <b>1.87</b> | 0.69        | <b>0.80</b> | 0.92 |                      | 30  | <b>0.97</b> | <b>0.94</b> | <b>1.11</b> | -0.08       | <b>0.12</b> | 0.84 |
|  | EMEP  | 37 | <b>0.89</b> | 1.53        | <b>1.28</b> | 0.34        | <b>0.18</b> | 0.94 |                      | 30  | <b>1.00</b> | <b>1.10</b> | <b>1.09</b> | <b>0.06</b> | <b>0.08</b> | 0.87 |
|  | LOTO  | 37 | <b>0.95</b> | <b>1.29</b> | <b>1.15</b> | <b>0.17</b> | <b>0.09</b> | 0.92 |                      | 30  | <b>0.80</b> | <b>0.71</b> | <b>1.25</b> | -0.43       | <b>0.41</b> | 0.87 |
|  | MATCH | 37 | <b>0.95</b> | 1.37        | <b>1.16</b> | <b>0.26</b> | <b>0.13</b> | 0.94 |                      | 30  | <b>0.93</b> | <b>1.16</b> | <b>1.16</b> | <b>0.05</b> | <b>0.09</b> | 0.87 |
|  | MINNI | 37 | <b>0.97</b> | <b>1.25</b> | <b>1.10</b> | <b>0.22</b> | <b>0.10</b> | 0.96 |                      | 30  | 0.10        | 0.31        | 5.11        | -0.95       | 1.58        | 0.89 |
| TNH4   | CHIM  | 39 | <b>0.85</b> | <b>1.17</b> | <b>1.21</b> | <b>0.27</b> | <b>0.37</b> | 0.87 | WNHx                 | 32  | 0.22        | 0.36        | <b>3.43</b> | -0.93       | 1.74        | 0.69 |
|  | CMAQ  | 39 | <b>0.82</b> | 1.47        | <b>1.35</b> | 0.44        | <b>0.57</b> | 0.83 |                      | 32  | <b>0.59</b> | 0.55        | <b>1.70</b> | -0.61       | <b>0.80</b> | 0.69 |
|  | EMEP  | 39 | <b>0.92</b> | <b>0.96</b> | <b>1.20</b> | <b>0.09</b> | <b>0.20</b> | 0.87 |                      | 32  | <b>0.88</b> | <b>0.77</b> | <b>1.25</b> | -0.24       | <b>0.27</b> | 0.75 |
|  | LOTO  | 39 | <b>0.90</b> | <b>1.19</b> | <b>1.20</b> | <b>0.24</b> | <b>0.37</b> | 0.84 |                      | 32  | <b>0.63</b> | 0.58        | <b>1.72</b> | -0.65       | <b>1.02</b> | 0.54 |
|  | MATCH | 39 | <b>0.87</b> | <b>0.86</b> | <b>1.23</b> | -0.03       | <b>0.17</b> | 0.87 |                      | 32  | <b>0.91</b> | <b>0.97</b> | <b>1.16</b> | -0.02       | <b>0.29</b> | 0.66 |
|  | MINNI | 39 | <b>0.90</b> | 1.39        | <b>1.27</b> | 0.37        | <b>0.44</b> | 0.86 |                      | 32  | 0.25        | 0.35        | <b>3.54</b> | -0.91       | 1.64        | 0.72 |
| TSO4   | CHIM  | 54 | <b>0.85</b> | <b>1.24</b> | <b>1.24</b> | <b>0.14</b> | <b>0.24</b> | 0.92 | WSOx                 | 56  | 0.25        | 0.36        | <b>3.46</b> | -1.05       | 2.94        | 0.77 |
|  | CMAQ  | 54 | 0.35        | 2.14        | <b>2.09</b> | 0.62        | <b>0.81</b> | 0.92 |                      | 56  | <b>0.84</b> | <b>0.99</b> | <b>1.29</b> | -0.16       | <b>0.40</b> | 0.70 |
|  | EMEP  | 54 | <b>0.89</b> | <b>1.19</b> | <b>1.20</b> | <b>0.17</b> | <b>0.25</b> | 0.92 |                      | 56  | <b>0.80</b> | 1.42        | <b>1.29</b> | 0.36        | <b>0.39</b> | 0.82 |
|  | LOTO  | 54 | <b>0.89</b> | <b>1.20</b> | <b>1.20</b> | <b>0.10</b> | <b>0.24</b> | 0.92 |                      | 56  | <b>0.91</b> | <b>0.83</b> | <b>1.20</b> | -0.18       | <b>0.32</b> | 0.79 |
|  | MATCH | 54 | <b>0.87</b> | <b>1.26</b> | <b>1.27</b> | <b>0.24</b> | <b>0.36</b> | 0.89 |                      | 56  | <b>0.86</b> | 1.47        | <b>1.26</b> | <b>0.30</b> | <b>0.24</b> | 0.87 |
|  | MINNI | 54 | <b>0.80</b> | 1.55        | <b>1.43</b> | 0.33        | <b>0.30</b> | 0.93 |                      | 56  | <b>0.55</b> | 0.50        | <b>2.09</b> | -0.56       | <b>0.80</b> | 0.79 |

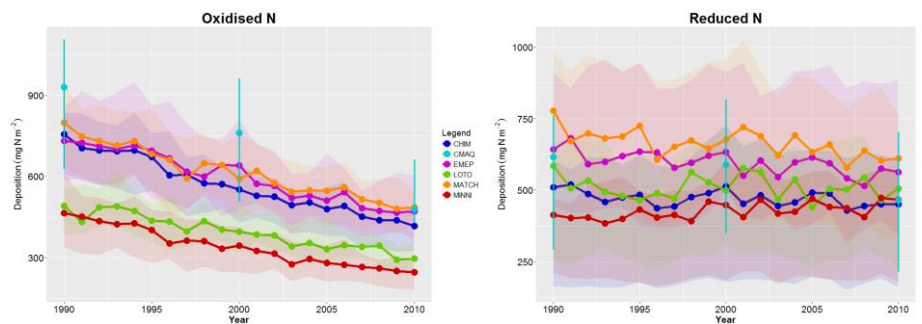


**Figure S26: Time series of modelled total deposition (wet plus dry) of oxidised N (left) and reduced N (right) at the measurement sites. Points represent the median value for all measurement sites and the shading (or error bars) represents the interquartile range.**

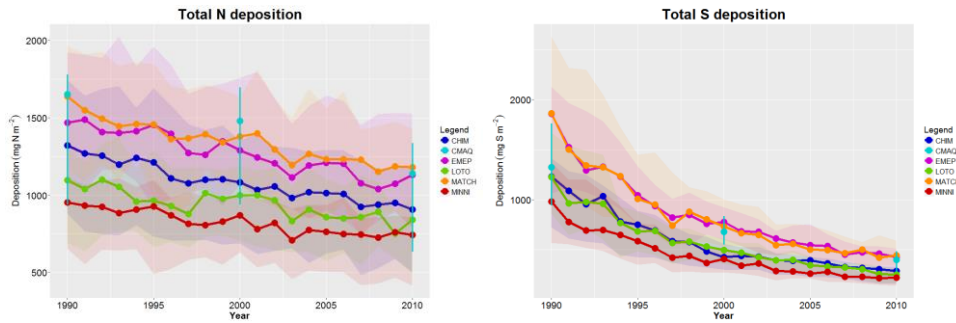


**Figure S27:** Time series of modelled total deposition (wet plus dry) of nitrogen (left) and sulphur (right) at the measurement sites. Points represent the median value for all measurement sites and the shading (or error bars) represents the interquartile range.

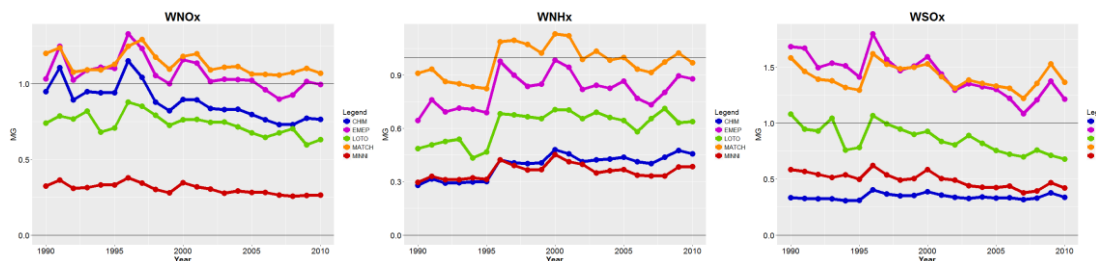


**Figure S28:** Time series of model geometric mean bias for WNOx, WNHx and WSOx.

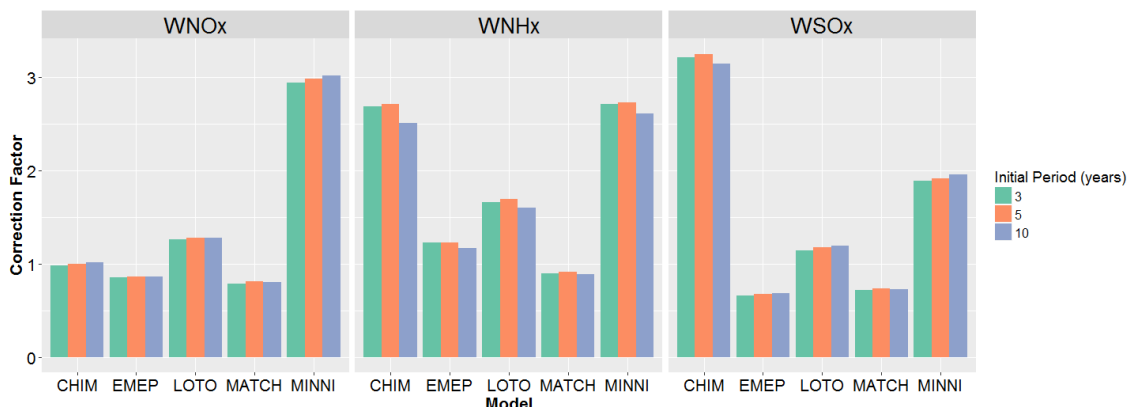


**Figure S29:** Bias correction factors for different lengths of initial period used for the bias correction.

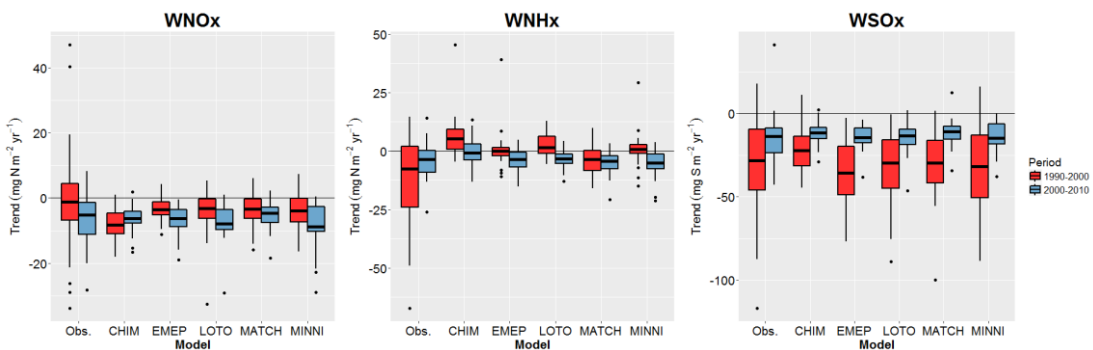


**Figure S30:** Tukey-style box plots of observed and bias-corrected (3 year initial period) modelled absolute trends for WNOx, WNHx, WSOx for the two periods 1990-2000 and 2000-2010.

## References cited in the Supplementary Material

- Andersson, C., Langner, J. and Bergström, R.: Interannual variation and trends in air pollution over Europe due to climate variability during 1958–2001 simulated with a regional CTM coupled to the ERA40 reanalysis, Tellus B, 59, 77-98, 2007.
- Banzhaf, S., Schaap, M., Kerschbaumer, A., Reimer, E., Stern, R., Van Der Swaluw, E. and Builtjes, P.: Implementation and evaluation of pH-dependent cloud chemistry and wet deposition in the chemical transport model REM-Calgrid, *Atmos. Environ.*, 49, 378-390, 2012.
- Berge, E.: Coupling of wet scavenging of sulphur to clouds in a numerical weather prediction model, *Tellus B*, 45, 1-22, 1993.
- Binkowski, F. S. and Shankar, U.: The regional particulate matter model: 1. Model description and preliminary results, *Journal of Geophysical Research: Atmospheres*, 100, 26191-26209, 1995.
- Byun, D. and Schere, K. L.: Review of the governing equations, computational algorithms, and other components of the Models-3 Community Multiscale Air Quality (CMAQ) modeling system, *Appl. Mech. Rev.*, 59, 51-77, 2006.
- Carter, W. P.: Documentation of the SAPRC-99 chemical mechanism for VOC reactivity assessment, Contract, 92, 95-308, 2000.
- Carter, W. P.: Condensed atmospheric photooxidation mechanisms for isoprene, *Atmos. Environ.*, 30, 4275-4290, 1996.
- Chang, J., Brost, R., Isaksen, I., Madronich, S., Middleton, P., Stockwell, W. and Walcek, C.: A three-dimensional Eulerian acid deposition model: Physical concepts and formulation, *Journal of Geophysical Research: Atmospheres*, 92, 14681-14700, 1987.
- Emberson, L., Simpson, D., Tuovinen, J., Ashmore, M. and Cambridge, H.: Towards a model of ozone deposition and stomatal uptake over Europe, *EMEP MSC-W Note*, 6, 1-57, 2000a.
- Emberson, L., Ashmore, M., Cambridge, H., Simpson, D. and Tuovinen, J.: Modelling stomatal ozone flux across Europe, *Environmental Pollution*, 109, 403-413, 2000b.
- Langner, J., Bergström, R. and Pleijel, K. 1998. European scale modelling of sulphur, oxidized nitrogen and photochemical oxidants. Model development and evaluation for the 1994 growing season, SMHI report, RMKNo. 82, Swedish Met. and Hydrol. Inst., Norrköping, Sweden
- Menut, L., Bessagnet, B., Khvorostyanov, D., Beekmann, M., Blond, N., Colette, A., Coll, I., Curci, G., Foret, G. and Hodzic, A.: CHIMERE 2013: a model for regional atmospheric composition modelling, *Geoscientific model development*, 6, 981-1028, 2013.
- Mozurkewich, M.: The dissociation constant of ammonium nitrate and its dependence on temperature, relative humidity and particle size, *Atmospheric Environment.Part A.General Topics*, 27, 261-270, 1993.
- Nenes, A., Pandis, S. N. and Pilinis, C.: Continued development and testing of a new thermodynamic aerosol module for urban and regional air quality models, *Atmos. Environ.*, 33, 1553-1560, 1999.
- Scott, B.: Parameterization of sulfate removal by precipitation, *J. Appl. Meteorol.*, 17, 1375-1389, 1978.
- Seinfeld, J. H. and Pandis, S. N.: From air pollution to climate change, *Atmospheric Chemistry and Physics*, John Wiley & Sons, New York, 1326, 1998.
- Simpson, D., Fagerli, H., Jonson, J., Tsyro, S. and Wind, P.: Transboundary Acidification, Eutrophication and Ground Level Ozone in Europe.Part I-Unified EMEP Model Description.Norwegian Meteorological Institute, Oslo, 2003.
- Simpson, D., Benedictow, A., Berge, H., Bergström, R., Emberson, L. D., Fagerli, H., Flechard, C. R., Hayman, G. D., Gauss, M. and Jonson, J. E.: The EMEP MSC-W chemical transport model—technical description, *Atmospheric Chemistry and Physics*, 12, 7825-7865, 2012.
- Strand, A. and Hov, Ø.: A two- dimensional global study of tropospheric ozone production, *Journal of Geophysical Research: Atmospheres*, 99, 22877-22895, 1994.
- Tuovinen, J., Ashmore, M., Emberson, L. and Simpson, D.: Testing and improving the EMEP ozone deposition module, *Atmos. Environ.*, 38, 2373-2385, 2004.
- Van Zanten, M., Sauter, F., RJ, W. K., Van Jaarsveld, J. and Van Pul, W.: Description of the DEPAC module: Dry deposition modelling with DEPAC\_GCN2010, RIVM rapport 680180001, 2010.
- Venkatram, A. and Pleim, J.: The electrical analogy does not apply to modeling dry deposition of particles, *Atmos. Environ.*, 33, 3075-3076, 1999.
- Walcek, C. J. and Taylor, G. R.: A theoretical method for computing vertical distributions of acidity and sulfate production within cumulus clouds, *J. Atmos. Sci.*, 43, 339-355, 1986.
- Wesely, M.: Parameterization of surface resistances to gaseous dry deposition in regional-scale numerical models, *Atmospheric Environment* (1967), 23, 1293-1304, 1989.
- Wichink Kruit, R., Schaap, M., Sauter, F., Van der Swaluw, E. and Weijers, E.: Improving the understanding of the secondary inorganic aerosol distribution over the Netherlands, *TNO Rep.TNO-060-UT-2012*, 334, 2012.
- Yarwood, G., Rao, S., Yocke, M. and Whitten, G.: Updates to the carbon bond chemical mechanism: CB05, Final report to the US EPA, RT-0400675, 8, 2005.
- Zhang, L., Gong, S., Padro, J. and Barrie, L.: A size-segregated particle dry deposition scheme for an atmospheric aerosol module, *Atmos. Environ.*, 35, 549-560, 2001.